
Universal Rate-Distortion-Perception Representations for Lossy Compression

George Zhang

Electrical and Computer Engineering
University of Toronto
gq.zhang@mail.utoronto.ca

Jingjing Qian

Electrical and Computer Engineering
McMaster University
qianj40@mcmaster.ca

Jun Chen

Electrical and Computer Engineering
McMaster University
chenjun@mcmaster.ca

Ashish Khisti

Electrical and Computer Engineering
University of Toronto
akhisti@ece.utoronto.ca

Abstract

In the context of lossy compression, Blau & Michaeli [5] adopt a mathematical notion of perceptual quality and define the information rate-distortion-perception function, generalizing the classical rate-distortion tradeoff. We consider the notion of universal representations in which one may fix an encoder and vary the decoder to achieve any point within a collection of distortion and perception constraints. We prove that the corresponding information-theoretic universal rate-distortion-perception function is operationally achievable in an approximate sense. Under MSE distortion, we show that the entire distortion-perception tradeoff of a Gaussian source can be achieved by a single encoder of the same rate asymptotically. We then characterize the achievable distortion-perception region for a fixed representation in the case of arbitrary distributions, and identify conditions under which the aforementioned results continue to hold approximately. This motivates the study of practical constructions that are approximately universal across the RDP tradeoff, thereby alleviating the need to design a new encoder for each objective. We provide experimental results on MNIST and SVHN suggesting that on image compression tasks, the operational tradeoffs achieved by machine learning models with a fixed encoder suffer only a small penalty when compared to their variable encoder counterparts.

1 Introduction

Unlike in lossless compression, the decoder in a lossy compression system has flexibility in how to reconstruct the source. Conventionally, some measure of distortion such as mean squared error, PSNR or SSIM/MS-SSIM [36, 37] is used as a quality measure. Accordingly, lossy compression algorithms are analyzed through rate-distortion theory, wherein the objective is to minimize the amount of distortion for a given rate. However, it has been observed that low distortion is not necessarily synonymous with high perceptual quality; indeed, deep learning based image compression has inspired works in which authors have noted that increased perceptual quality may come at the cost of increased distortion [1, 4]. This culminated in the work of Blau & Michaeli [5] who propose the rate-distortion-perception theoretical framework.

The main idea was to introduce a third *perception* axis which more closely mimics what humans would deem to be visually pleasing. Unlike distortion, judgement of perceptual quality is taken to

be inherently no-reference. The mathematical proxy for perceptual quality then comes in the form of a divergence between the source and the reconstruction *distributions*, motivated by the idea that perfect perceptual quality is achieved when they are identical. Leveraging generative adversarial networks [11] in the training procedure has made such a task possible for complex data-driven settings with efficacy even at very low rates [33]. Naturally, this induces a tradeoff between optimizing for perceptual quality and optimizing for distortion. But in designing a lossy compression system, one may wonder where exactly this tradeoff lies: is the objective tightly coupled with optimizing the representations generated by the encoder, or can most of this tradeoff be achieved by simply changing the decoding scheme?

Our contributions are as follows. We define the notion of *universal* representations which are generated by a fixed encoding scheme for the purpose of operating at multiple perception-distortion tradeoff points attained by varying the decoder. We then prove a coding theorem establishing the relationship between this operational definition and an information universal rate-distortion-perception function. Under MSE distortion loss, we study this function for the special case of the Gaussian distribution and show that the penalty in fixing the representation map with fixed rate can be small in many interesting regimes. For general distributions, we characterize the achievable distortion-perception region with respect to an arbitrary representation and establish a certain approximate universality property.

We then turn to study how the operational tradeoffs achieved by machine learning models on image compression under a fixed encoder compared to varying encoders. Our results suggest that there is not much loss in reusing encoders trained for a specific point on the distortion-perception tradeoff across other points. The practical implication of this is to reduce the number of models to be trained within deep-learning enhanced compression systems. Building on [30, 31], one of the key steps in our techniques is the assumption of *common randomness* between the sender and receiver which will turn out to reduce the coding cost. Throughout this work, we focus on the scenario where a rate is fixed in advance. We address the scenario when the rate is changed in the supplementary.

2 Related Works

Image quality measures include full-reference metrics (which require a ground truth as reference), or no-reference metrics (which only use statistical features of inputs). Common full-reference metrics include MSE, SSIM/MS-SSIM [36, 37], PSNR or deep feature based distances [16, 41]. No-reference metrics include BRISQUE/NIQE/PIQE [23, 24, 35] and Fréchet Inception Distance [14]. Roughly speaking, one can consider the former set to be distortion measures and the latter set to be perception measures in the rate-distortion-perception framework. Since GANs capable of synthesizing highly realistic samples have emerged, using trained discriminators as a proxy for perceptual quality in deep learning based systems has also been explored [17]. This idea is principled as various GAN objectives can be interpreted as estimating particular statistical distances [3, 25, 26].

Rate-distortion theory has long served as a theoretical foundation for lossy compression [7]. Within machine learning, variations of rate-distortion theory have been introduced to address representation learning [2, 6, 34], wherein a central task is to extract useful information from data on some sort of budget, and also in the related field of generative modelling [15]. On the other hand, distribution-preserving lossy compression problems have also been studied in classical information theory literature [27, 28, 40].

More recently, in an effort to reduce blurriness and other artifacts, machine learning research in lossy compression has attempted to incorporate GAN regularization into compressive autoencoders [1, 5, 33], which were traditionally optimized only for distortion loss [21, 32]. This has led to highly successful data-driven models operating at very low rates, even for high-resolution images [22]. An earlier work of Blau & Michaeli [4] studied only the perception-distortion tradeoff within deep learning enhanced image restoration using GANs. This idea was then incorporated with distribution-preserving lossy compression [33] to study the rate-distortion-perception tradeoff in full generality [5].

The work most similar to ours is [39], who observe that an optimal encoder for the “classic” rate-distortion function is also optimal for perfect perceptual compression at twice the distortion. Our work investigates the intermediate regime and also includes common randomness as a modelling

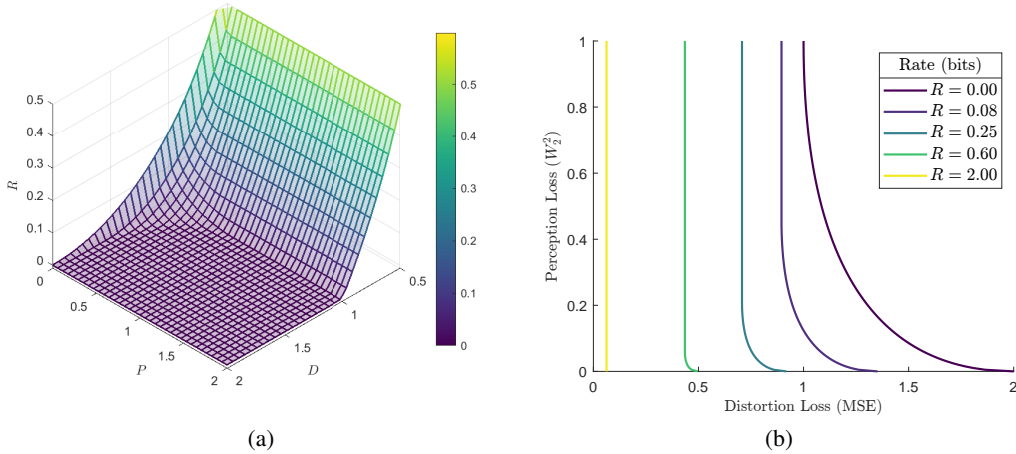


Figure 1: (a) The information Rate-Distortion-Perception function $R(D, P)$ for a standard Gaussian source X . (b) Distortion-perception cross-sections across multiple rates. The tension between perception and distortion is most visible at low rates. When both P and D are active, Theorem 3 implies that the rate needed to achieve an entire cross-section along fixed rate is the same as the rate to achieve any single point on the cross-section in the asymptotic setting.

assumption, which in principle allows us to achieve perfect perceptual quality at lower than twice the distortion. The concurrent work [10] also establishes the achievable distortion-perception region as in our Theorem 4 and provides a geometric interpretation of the optimal interpolator in Wasserstein space.

3 Rate-Distortion-Perception Representations

The backbone of rate-distortion theory characterizes an (operational) objective expressing what can be achieved by encoders and decoders with a quantization bottleneck in terms of an *information* function which is more convenient to analyze. Let $X \sim p_X$ be an information source to be compressed through quantization. The quality of the compressed source is measured by a distortion function $\Delta : \mathcal{X} \times \mathcal{X} \rightarrow \mathbb{R}_{\geq 0}$ satisfying $\Delta(x, \hat{x}) = 0$ if and only if $x = \hat{x}$. We distinguish between the *one-shot* scenario in which we compress one symbol at a time, and the *asymptotic* scenario in which we encode n i.i.d. samples from X jointly and analyze the behaviour as $n \rightarrow \infty$. The minimum rate needed to meet the distortion constraint D on average is denoted by $R^*(D)$ in the one-shot setting and by $R^{(\infty)}(D)$ in the asymptotic setting. These are studied through the information rate-distortion function

$$R(D) = \inf_{p_{\hat{X}|X}} I(X; \hat{X}) \quad \text{s.t.} \quad \mathbb{E}[\Delta(X, \hat{X})] \leq D, \quad (1)$$

where $I(X; \hat{X})$ is the mutual information between a source X and reconstruction \hat{X} . The principal result of rate-distortion theory states that $R^{(\infty)}(D) = R(D)$ [7]. Furthermore, it is also possible to characterize $R^*(D)$ using $R(D)$ as we will soon see.

In light of the discussion on perceptual quality, the flexibility in distortion function is not necessarily a good method to capture how realistic the output may be perceived. To resolve this, Blau & Michaeli [5] introduce an additional constraint to match the distributions of X and \hat{X} in the form of a non-negative divergence between probability measures $d(\cdot, \cdot)$ satisfying $d(p, q) = 0$ if and only if $p = q$. The one-shot rate-distortion-perception function $R^*(D, P)$ and asymptotic rate-distortion-perception function $R^{(\infty)}(D, P)$ are defined in the same fashion as their rate-distortion counterparts, which we will later make precise.

Definition 1 (iRDPF). The information rate-distortion-perception function for a source X is defined as

$$R(D, P) = \inf_{p_{\hat{X}|X}} I(X; \hat{X}) \\ \text{s.t.} \quad \mathbb{E}[\Delta(X, \hat{X})] \leq D, \quad d(p_X, p_{\hat{X}}) \leq P.$$

The strong functional representation lemma [19, 31] establishes relationships between the operational and information functions:

$$R^{(\infty)}(D, P) = R(D, P), \quad (2)$$

$$R(D, P) \leq R^*(D, P) \leq R(D, P) + \log(R(D, P) + 1) + 5. \quad (3)$$

These results hold also for $R(D) = R(D, \infty)$. We make note that they were developed under a more general set of constraints for which stochastic encoders and decoders with a shared source of randomness were used. In practice, the sender and receiver agree on a random seed beforehand to emulate this behaviour.

3.1 Gaussian Case

We now present the closed form expression of $R(D, P)$ for a Gaussian source under MSE distortion and squared Wasserstein-2 perception losses (see also Figure 1(a) and Figure 1(b)). Recall that the squared Wasserstein-2 distance is defined as

$$W_2^2(p_X, p_{\hat{X}}) = \inf \mathbb{E}[\|X - \hat{X}\|^2], \quad (4)$$

where the infimum is over all joint distributions of (X, \hat{X}) with marginals p_X and $p_{\hat{X}}$. Let $\mu_X = \mathbb{E}[X]$ and $\sigma_X^2 = \mathbb{E}[\|X - \mu_X\|^2]$.

Theorem 1. *For a scalar Gaussian source $X \sim \mathcal{N}(\mu_X, \sigma_X^2)$, the information rate-distortion-perception function under squared error distortion and squared Wasserstein-2 distance is attained by some \hat{X} jointly Gaussian with X and is given by*

$$R(D, P) = \begin{cases} \frac{1}{2} \log \frac{\sigma_X^2 (\sigma_X - \sqrt{P})^2}{\sigma_X^2 (\sigma_X - \sqrt{P})^2 - (\frac{\sigma_X^2 + (\sigma_X - \sqrt{P})^2 - D}{2})^2} & \text{if } \sqrt{P} \leq \sigma_X - \sqrt{|\sigma_X^2 - D|}, \\ \max\{\frac{1}{2} \log \frac{\sigma_X^2}{D}, 0\} & \text{if } \sqrt{P} > \sigma_X - \sqrt{|\sigma_X^2 - D|}. \end{cases}$$

When $\sqrt{P} > \sigma_X - \sqrt{|\sigma_X^2 - D|}$, the perception constraint is inactive and $R(D, P) = R(D)$. The choice of $W_2^2(\cdot, \cdot)$ perception loss turns out to not be essential; we show in the supplementary that $R(D, P)$ can also be expressed under the KL-divergence.

3.2 Universal Representations

Whereas the RDP function is regarded as the minimal rate for which we can vary an encoder-decoder pair to meet any distortion and perception constraints (D, P) , the universal RDP (uRDP) function generalizes this to the case where we fix an encoder and allow only the decoder to adapt in order to meet multiple constraints $(D, P) \in \Theta$. For example, one case of interest is when Θ is the set of all (D, P) pairs associated with a given rate along the iRDP function; how much additional rate is needed if this is to be achieved by a fixed encoder, rather than varying it across each objective? The hope is that the rate to use some fixed encoder across this set is not much larger than the rate to achieve any single point. As we will see for the Gaussian distribution, this is in fact the case in the asymptotic setting, and also approximately true in the one-shot setting. Below, we define the one-shot universal rate-distortion-perception function and the information universal rate-distortion-perception function, then establish a relationship between the two. In these definitions we assume X is a random variable and Θ is an arbitrary non-empty set of (D, P) pairs.

Definition 2 (ouRDPF). A Θ -universal encoder of rate R is said to exist if we can find random variable U , encoding function $f_U : \mathcal{X} \rightarrow \mathcal{C}_U$ and decoding functions $g_{U,D,P} : \mathcal{C}_U \rightarrow \hat{\mathcal{X}}$, $(D, P) \in \Theta$ such that

$$\mathbb{E}[\ell(f_U(X))] \leq R, \quad \mathbb{E}[\Delta(X, \hat{X}_{D,P})] \leq D, \quad d(p_X, p_{\hat{X}_{D,P}}) \leq P,$$

where \mathcal{C}_U is a uniquely decodable binary code specified by U , $\hat{X}_{D,P} = g_{U,D,P}(f_U(X))$, and $\ell(f_U(X))$ denotes the length of binary codeword $f_U(X)$. The random variable U acts as a shared source of randomness. The infimum of such R is called the one-shot universal rate-distortion-perception function (ouRDPF) and denoted by $R^*(\Theta)$. When $\Theta = \{(D, P)\}$, this specializes to the one-shot rate-distortion-perception function $R^*(D, P)$.

Definition 3 (iuRDPF). Let Z be a representation of X (i.e. generated by some random transform $p_{Z|X}$). Let $\mathcal{P}_{Z|X}(\Theta)$ be the set of transforms $p_{Z|X}$ such that for each $(D, P) \in \Theta$, there exists $p_{\hat{X}_{D,P}|Z}$ for which

$$\mathbb{E}[\Delta(X, \hat{X}_{D,P})] \leq D \text{ and } d(p_X, p_{\hat{X}_{D,P}}) \leq P,$$

where $X \leftrightarrow Z \leftrightarrow \hat{X}_{D,P}$ are assumed to form a Markov chain. Define

$$R(\Theta) = \inf_{p_{Z|X} \in \mathcal{P}_{Z|X}(\Theta)} I(X; Z). \quad (5)$$

We refer to this as the information universal rate-distortion-perception function (iuRDPF) and say that the random variable Z is a representation which is Θ -universal with respect to X . The conditional distributions $p_{\hat{X}_{D,P}|Z}$ induce stochastic mappings transforming the representations to reconstructions $\hat{X}_{D,P}$ in order to meet specific (D, P) constraints.

Note that we assume a shared source of stochasticity within the ouRDPF as a tool to prove the achievability of the iuRDPF, but not within the definition of the iuRDPF itself. Moreover, source X , reconstruction $\hat{X}_{D,P}$, representation Z , and random seed U are all allowed to be multivariate random variables.

Theorem 2. $R(\Theta) \leq R^*(\Theta) \leq R(\Theta) + \log(R(\Theta) + 1) + 5$.

In practice, the overhead $\log(R(\Theta) + 1) + 5$ either makes the upper bound an overestimate of $R^*(\Theta)$ or is negligible compared to $R(\Theta)$. This overhead vanishes completely in the asymptotic setting as we will show in the supplementary. We can therefore interpret $R(\Theta)$ as the rate required to meet an entire set Θ of constraints with the encoder fixed. Within the set Θ , it is clear that $\sup_{(D,P) \in \Theta} R(D, P)$ characterizes the rate required to meet the most demanding constraint. Now define

$$A(\Theta) = R(\Theta) - \sup_{(D,P) \in \Theta} R(D, P), \quad (6)$$

which is the rate penalty incurred by meeting *all* constraints in Θ with the encoder fixed. Let $\Omega(R) = \{(D, P) : R(D, P) \leq R\}$. It is ideal to have $A(\Omega(R)) = 0$ for each R so that achieving the entire tradeoff with a single encoder is essentially no more expensive than to achieve any single point on the tradeoff, thereby alleviating the need to design a host of encoders for different distortion-perception objectives with respect to the same rate.

One can also take the following alternative perspective. The proof of Theorem 2 shows that every representation Z can be generated from source X using an encoder of rate $I(X; Z) + o(I(X; Z))$, and based on Z , the decoder can produce reconstruction $\hat{X}_{D,P}$ by leveraging random seed U to simulate conditional distribution $p_{\hat{X}_{D,P}|Z}$. Therefore, the problem of designing an encoder boils down to identifying a suitable representation. Given a representation Z of X , we define the achievable distortion-perception region $\Omega(p_{Z|X})$ as the set of all (D, P) pairs for which there exists $p_{\hat{X}_{D,P}|Z}$ such that $\mathbb{E}[\Delta(X, \hat{X}_{D,P})] \leq D$ and $d(p_X, p_{\hat{X}_{D,P}}) \leq P$. Intuitively, $\Omega(p_{Z|X})$ is the set of all possible distortion-perception constraints that can be met based on representation Z . If $\Omega(p_{Z|X}) = \Omega(R)$ for some representation Z with $I(X; Z) = R$, then Z has the maximal achievable distortion-perception region in the sense that $\Omega(p_{Z'|X}) \subseteq \Omega(p_{Z|X})$ for any Z' with $I(X; Z') \leq R$. In the supplementary material we establish mild regularity conditions for which the existence of such Z is equivalent to the aforementioned desired property $A(\Omega(R)) = 0$. We shall show that that this ideal scenario actually arises in the Gaussian case and an approximate version can be found more broadly.

Theorem 3. Let $X \sim \mathcal{N}(\mu_X, \sigma_X^2)$ be a scalar Gaussian source and assume MSE and $W_2^2(\cdot, \cdot)$ losses. Let Θ be any non-empty set of (D, P) pairs. Then

$$A(\Theta) = 0. \quad (7)$$

Moreover, for any representation Z jointly Gaussian with X such that

$$I(X; Z) = \sup_{(D,P) \in \Theta} R(D, P), \quad (8)$$

we have

$$\Theta \subseteq \Omega(p_{Z|X}) = \Omega(I(X; Z)). \quad (9)$$

Next we consider a general source $X \sim p_X$ and characterize the achievable distortion-perception region for an arbitrary representation Z under MSE loss. We then provide some evidence indicating that every reconstruction $\hat{X}_{D,P}$ achieving some point (D, P) on the distortion-perception tradeoff for a given R likely has the property $\Omega(p_{\hat{X}_{D,P}|X}) \approx \Omega(R)$.

Theorem 4 (Approximate universality for general sources). *Assume MSE loss and any perception measure $d(\cdot, \cdot)$. Let Z be any arbitrary representation of X . Then*

$$\Omega(p_{Z|X}) \subseteq \left\{ (D, P) : D \geq \mathbb{E}[\|X - \tilde{X}\|^2] + \inf_{p_{\tilde{X}}: d(p_X, p_{\tilde{X}}) \leq P} W_2^2(p_{\tilde{X}}, p_X) \right\} \subseteq \text{cl}(\Omega(p_{Z|X})),$$

where $\tilde{X} = \mathbb{E}[X|Z]$ is the reconstruction minimizing squared error distortion with X under the representation Z and $\text{cl}(\cdot)$ denotes set closure. In particular, the two extreme points $(D^{(a)}, P^{(a)}) = (\mathbb{E}[\|X - \tilde{X}\|^2], d(p_X, p_{\tilde{X}}))$ and $(D^{(b)}, P^{(b)}) = (\mathbb{E}[\|X - \tilde{X}\|^2] + W_2^2(p_{\tilde{X}}, p_X), 0)$ are contained in $\text{cl}(\Omega(p_{Z|X}))$.

To gain a better understanding, let Z be an optimal reconstruction $\hat{X}_{D,P}$ associated with some point (D, P) on the distortion-perception tradeoff for a given R , i.e., $I(X; \hat{X}_{D,P}) = R(D, P) = R$ (assuming that D and/or P cannot be decreased without violating $R(D, P) = R$), $\mathbb{E}[\|X - \hat{X}_{D,P}\|^2] = D$, $d(p_X, p_{\hat{X}_{D,P}}) = P$. We assume for simplicity that $\hat{X}_{D,P}$ exists for every (D, P) on the tradeoff. Such (D, P) is on the boundary of $\text{cl}(\Omega(p_{\hat{X}_{D,P}|X}))$. Theorem 4 indicates that $\text{cl}(\Omega(p_{\hat{X}_{D,P}|X}))$ contains two extreme points: the upper-left $(D^{(a)}, P^{(a)})$ and the lower-right $(D^{(b)}, P^{(b)})$. Under the assumption that $d(\cdot, \cdot)$ is convex in its second argument, $\text{cl}(\Omega(p_{\hat{X}_{D,P}|X}))$ is a convex region containing the aforementioned points.

Figure 2 illustrates $\Omega(R)$ and $\Omega(p_{\hat{X}_{D,P}|X})$ for several different choices of (D, P) . When $R = 0$, $\Omega(p_{\hat{X}_{D,P}|X}) = \Omega(R)$ for any such $\hat{X}_{D,P}$. So we have $\Omega(p_{\hat{X}_{D,P}|X}) \approx \Omega(R)$ in the low-rate regime where the tension between distortion and perception is most visible. More general quantitative results are provided in the supplementary. Let $\sigma_X^2 = \mathbb{E}[\|X - \mathbb{E}[X]\|^2]$. If \hat{X}_{D_1, P_1} is chosen to be the optimal reconstruction in the conventional rate-distortion sense associated with point (D_1, P_1) , then the upper-left extreme points of $\Omega(p_{\hat{X}_{D_1, P_1}|X})$ and $\Omega(R)$ coincide (i.e., $(D^{(a)}, P^{(a)}) = (D_1, P_1)$) and the lower-right extreme points of $\Omega(p_{\hat{X}_{D_1, P_1}|X})$ and $\Omega(R)$ (i.e., $(D^{(b)}, 0)$ and $(D_3, 0)$ with $R(D_3, 0) = R(D_1, \infty)$) must be close to each other in the sense that

$$\frac{1}{2}\sigma_X^2 \geq D^{(b)} - D_3 \stackrel{D_1 \approx 0 \text{ or } \sigma_X^2}{\approx} 0, \quad 2 \geq \frac{D^{(b)}}{D_3} \stackrel{D_1 \approx \sigma_X^2}{\approx} 1, \quad (10)$$

which suggests that $\Omega(p_{\hat{X}_{D_1, P_1}|X})$ is not much smaller than $\Omega(R)$. Moreover, in this case we have

$$D^{(b)} \leq 2\mathbb{E}[\|X - \tilde{X}\|^2] \leq 2D_1, \quad (11)$$

which implies that $(2D_1, 0)$ is dominated by extreme point $(D^{(b)}, 0)$ and consequently must be contained in $\text{cl}(\Omega(p_{\hat{X}_{D_1, P_1}|X}))$. Therefore, the optimal representation in the conventional rate-distortion sense can be leveraged to meet any perception constraint with no more than a two-fold increase in distortion. As a corollary, one recovers Theorem 2 in Blau & Michaeli ($R(2D, 0) \leq$

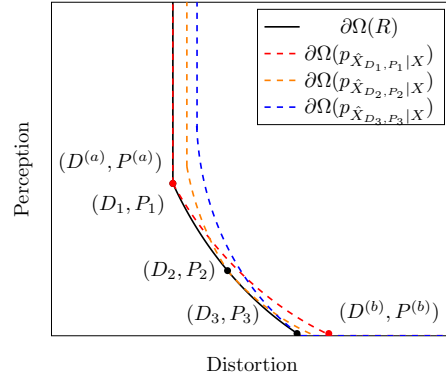


Figure 2: Approximate universality for a general source. Illustrated are boundaries of achievable distortion-perception regions for three representations: minimal distortion (D_1, P_1) for $R(D_1, P_1) = R(D_1, \infty)$, midpoint (D_2, P_2) , and perfect perceptual quality (D_3, P_3) where $P_3 = 0$. We have $\Omega(p_{\hat{X}_{D_i, P_i}|X}) \approx \Omega(R)$, especially when R is small. The extreme points $(D^{(a)}, P^{(a)})$ and $(D^{(b)}, P^{(b)})$ for \hat{X}_{D_1, P_1} are shown. $(D^{(a)}, P^{(a)})$ coincides with (D_1, P_1) .

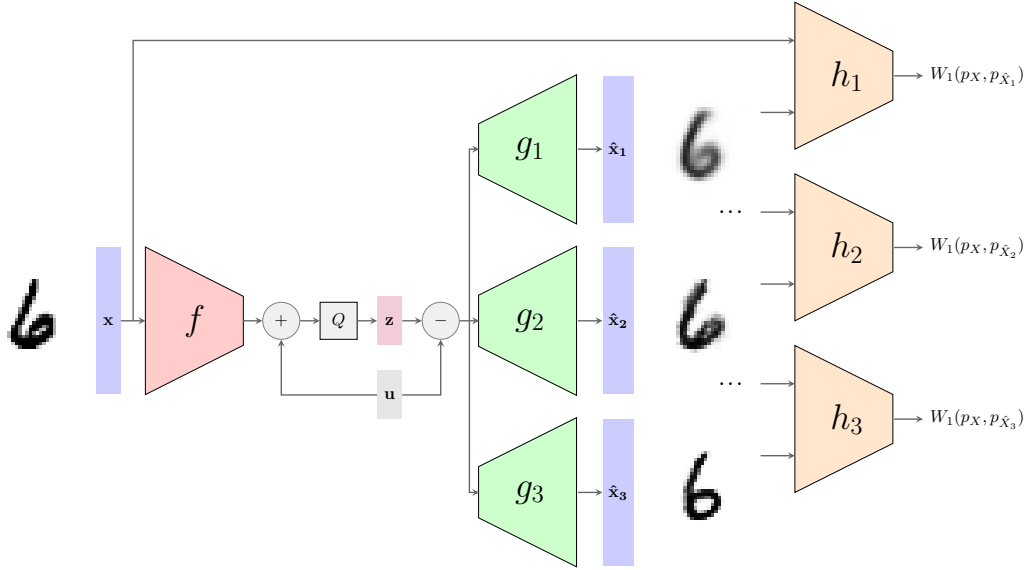


Figure 3: An illustration of the experimental setup for the universal model. A single encoder f is trained for an initial perception-distortion tradeoff and has its weights frozen. Subsequently many other decoders $\{g_i\}$ are optimized for different tradeoff points using the representations z produced by f . The sender and receiver have access to a shared source of randomness u for universal quantization [30, 42]. Q denotes the quantizer. Separate critic networks $\{h_i\}$ are trained along with each decoder to promote perceptual quality. In this figure, the top decoder places most weight on distortion loss whereas the bottom decoder places most weight on perceptual loss. This has the effect of reducing the blurriness, but comes at the cost of a less faithful reconstruction of the original (in extreme cases even changing the identity of the digit). The perception losses $W_1(p_X, p_{\hat{x}_i})$ are estimated using the critics $\{h_i\}$ by replacing the expectations in Equation (14) with samples from the test set.

$R(D, \infty)$). Hence, the numerical connection between $R(2D, 0)$ and $R(D, \infty)$ is a manifestation of the existence of approximately $\Omega(I(X; Z))$ -universal representations Z . These analyses motivate the study of practical constructions for which we seek to achieve multiple (D, P) pairs with a single encoder.

3.3 Successive Refinement

Up until now, we have established the notion of distortion-perception universality for a given rate. We can paint a more complete picture by extending this universality along the rate axis as well, known classically as successive refinement [9] when restricted to the rate-distortion function. Informally, given two sets of (D, P) pairs Θ_1 and Θ_2 , we say that rate pair (R_1, R_2) is (operationally) *rate-distortion-perception refinable* if there exists a base encoder optimal for $R(\Theta_1)$ which, when combined with a second refining encoder, is also optimal for $R(\Theta_2)$. In other words, bits are transmitted in two stages and each stage achieves optimal rate-distortion-perception performance. This nice property is not true of general distributions but we show in supplementary section A.3 that it holds in the asymptotic Gaussian case, thus generalizing Theorem 3. Nonetheless, building on [18] we prove an approximate refinability property of general distributions and in section B.3 provide experimental results demonstrating approximate refinability on image compression using deep learning.

4 Experimental Results

The rate-distortion-perception tradeoff was observed as a result of applying GAN regularization within deep-learning based image compression [5, 33]. Therein, an entire end-to-end model is trained for each desired setting over rate, distortion, and perception. In practice it is undesirable to develop an entire system from scratch for each objective and we would like to reuse trained networks with

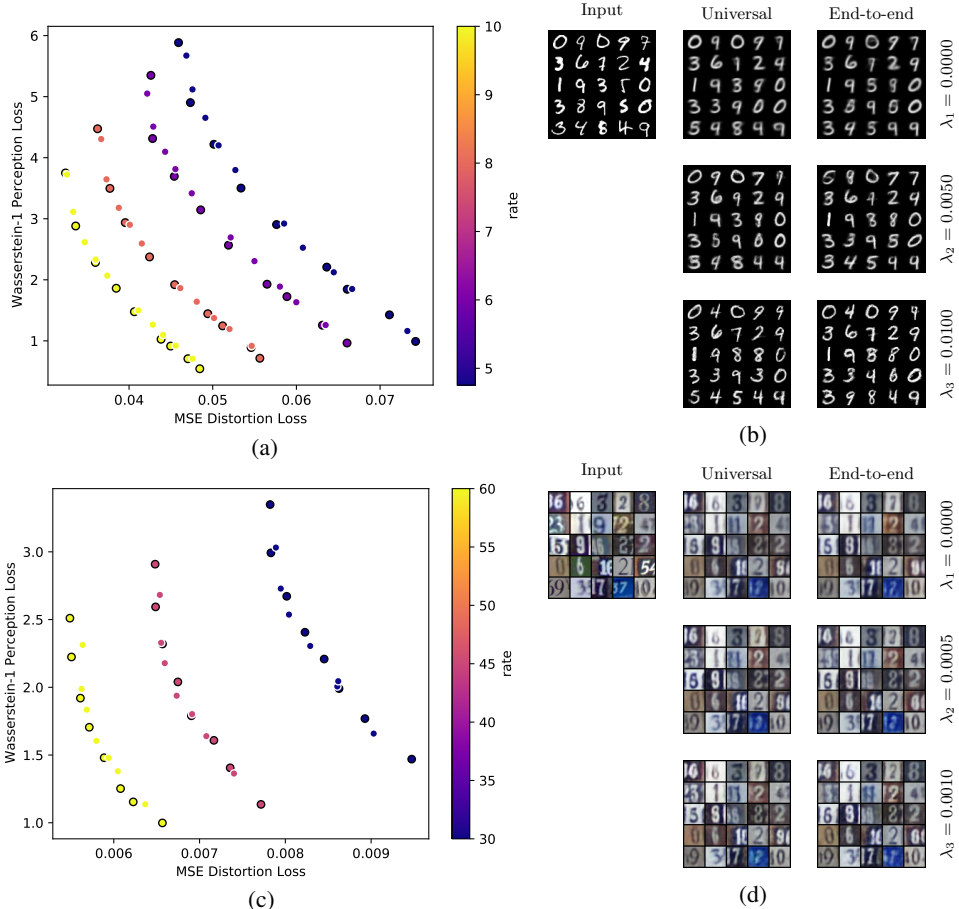


Figure 4: (a) (c) Rate-distortion-perception tradeoffs along various rates. Points with black outline are losses reported for the end-to-end encoder-decoder pairs trained jointly for a particular perception-distortion objective. Other points are the losses for universal models, in which decoders are trained over a frozen encoder optimized for small P (MNIST: $\lambda = 0.015$, SVHN: $\lambda = 0.002$). Universal model performance is very close to performance of end-to-end models across all tradeoffs $\{\lambda_i\}$. (b) (d) Outputs of selected models (MNIST: $R = 6$, SVHN: $R = 60$). As the emphasis on perception loss λ_i increases, the outputs become sharper. The visual quality of both the end-to-end and universal models are on average comparable for each λ_i . More experiment details are given in the supplementary.

frozen weights if possible. It is of interest to assess the distortion and perception penalties incurred by such model reuse, most naturally in the scenario of fixing a pre-trained encoder.

Concretely, we refer to models where the encoder and decoder are trained jointly for an objective as *end-to-end* models, and models for which some encoder is fixed in advance as (approximately) *universal* models. The encoders used within the universal models are borrowed from the end-to-end models, and the choice of which to use will be discussed later in this section. Within the same dataset, universal models and end-to-end models using the same hyperparameter settings differ only in the trainability of the encoder.

4.1 Setup and Training

The architecture we use is a stochastic autoencoder with GAN regularization, wherein a single model consists of an encoder f , a decoder g , and a critic h . Details about the networks can be found in the supplementary; here, we summarize first the elements relevant to facilitating compression then the training procedure. Let x be an input image. The final layer of the encoder consists of a tanh activation to produce a symbol $f(x) \in [-1, 1]^d$, with the intent to divide this into L -level intervals of uniform length $2/(L - 1)$ across d dimensions for some L . This gives an upper bound

of $d \log(L)$ for the model rate, and it was found to be only slightly suboptimal by Agustsson et al. [1]; we found the estimate to be off by at most 6% on MNIST. To achieve high perceptual quality through generative modelling, stochasticity is necessary¹ [33]. In accordance with the shared randomness assumption within the ouRDPF, our main experimental results use the universal/dithered quantization² [12, 29, 30, 42] scheme where the sender and receiver both have access to a sample $u \sim U[-1/(L-1), +1/(L-1)]^d$. The sender computes

$$z = \text{Quantize}(f(x) + u) \quad (12)$$

and gives z to the receiver. The receiver then reconstructs the image by feeding $z - u$ to the decoder. The soft gradient estimator of [21] is used to backpropagate through the quantizer. Compared to alternate schemes where noise is added only at the decoder, this scheme has the advantage of reducing the quantization error by centering it around $f(x)$ and can be emulated on the agreement of a random seed. Since this is not always possible in practice, the results for a more restrictive quantization scheme where the sender and receiver do not have access to common randomness are included in Figure 5 in the supplementary.

The rest of the design follows closely the design of Blau & Michaeli [5]. We first produce the end-to-end models, in which f, g and h are all trainable. We use MSE loss for the distortion metric and estimate the Wasserstein-1 perception metric. The loss function is given by

$$\mathcal{L} = \mathbb{E}[\|X - \hat{X}\|^2] + \lambda W_1(p_X, p_{\hat{X}}), \quad (13)$$

where $p_{\hat{X}}$ is the reconstruction distribution induced by passing X through f , transmitting the representations via (12) then subtracting the noise and decoding through g . The particular tradeoff point achieved by the model is controlled by the weight λ . Kantorovich-Rubinstein duality allows us to write the Wasserstein-1 distance as

$$W_1(p_X, p_{\hat{X}}) = \max_{h \in \mathcal{F}} \mathbb{E}[h(X)] - \mathbb{E}[h(\hat{X})], \quad (14)$$

which expresses the objective as a min-max problem and allows us to treat it using GANs. Here, \mathcal{F} is the set of all bounded 1-Lipschitz functions. In practice, this class is limited by the discriminator architecture and the Lipschitz condition is approximated with a gradient penalty [13] term. Optimization alternates between minimizing over f, g with h fixed and maximizing over h with f, g fixed. In essence, g is trained to produce reconstructions that are simultaneously low distortion and high perception, so it acts as both a decoder and a generator. The reported perception loss is estimated using Equation (14) through test set samples. Figure 3 provides an overview of the entire scheme.

After the end-to-end models are trained, their encoders can be lent to construct universal models. The parameters of f are frozen we introduce a new decoder g_1 and critic h_1 trained to minimize

$$\mathcal{L}_1 = \mathbb{E}[\|X - \hat{X}_1\|^2] + \lambda_1 W_1(p_X, p_{\hat{X}_1}),$$

where λ_1 is another tradeoff parameter and $p_{\hat{X}_1}$ is the new reconstruction distribution. The weights of g_1 are initialized from random while the weights of h_1 are initialized from h . This was done for stability and faster convergence but in practice, we found that initializing from random performed just as well given sufficient iterations. The rest of the training procedure follows that of the first stage. This second stage is repeated over many different parameters $\{\lambda_i\}$ to generate a tradeoff curve. Further model and experimental details can be found in the supplementary material.

4.2 Results

Figure 4 shows rate-distortion-perception curves at multiple rates on MNIST and SVHN, obtained by varying λ from 0 to a selected upper bound for which training with the given hyperparameters remained stable. Note that the rate for each individual curve is fixed through using the same quantizer across all models. As the rate is increased by introducing better quantizers, optimizing for distortion loss has the side effect of reducing perception loss. The rates are thus chosen to be low as the tension between distortion and perception is most visible then. The points outlined in black are losses for end-to-end models and the other points correspond to the universal models sharing an encoder trained

¹This prevents us from passing noiseless quantized representations to the decoder.

²The use of the word "universal" here is unrelated to our notion of "universality".

from the end-to-end models. As can be seen, the universal models are able to achieve a tradeoff which is very close to the end-to-end models (with outputs that are visually comparable) despite operating with a fixed encoder.

For any fixed rate, decreasing the perception loss P induces outputs which are less blurry, at the cost of a reconstruction which is less faithful to the original input. This is especially evident at very low rates in which the compression system appears to act as a generative model. However, our experiments indicate that an encoder trained for small P can also be used to produce a low-distortion reconstruction by training a new decoder. Conversely, training a decoder to produce reconstructions with high perceptual quality on top of an encoder trained only for distortion loss is also possible as the decoder is sufficiently expressive to act purely as a generative model.

5 Discussion

Limitations. One limitation of these experiments is that we can slightly reduce the distortion loss by using deterministic nearest neighbour quantization rather than universal quantization, but there would no longer be stochasticity to train the generative model. A comparison of quantization schemes for the case of $\lambda = 0$ can be found in Table 1 of the supplementary. It may be beneficial to employ more sophisticated quantization schemes and explore losses beyond MSE as well.

Potential Negative Societal Impacts. The goal of our work is to advance perceptually-driven lossy compression, which conflicts with optimizing for distortion. We presume that this will be harmless in most multimedia applications but where reconstructions are used for classification or anomaly detection this may cause problems. For example, a low-rate face reconstruction deblurred by a GAN may lead to false identity recognition.

6 Conclusion

The use of deep generative models in data compression has highlighted the tradeoff between optimizing for low distortion and high perceptual quality. Previous works have designed end-to-end systems in order to achieve points across this tradeoff. Our results suggest that this may not be necessary, in that fixing a good representation map and varying only the decoder is sufficient for image compression in practice. We have also established a theoretical framework to study this scheme and characterized its limits, giving bounds for the case of specific distributions and loss functions. Future work includes evaluating the scheme on more diverse architectures, as well as employing the scheme to high-resolution images and videos.

References

- [1] Eirikur Agustsson, Michael Tschannen, Fabian Mentzer, Radu Timofte, and Luc Van Gool. Generative adversarial networks for extreme learned image compression. In *Proceedings of the IEEE International Conference on Computer Vision*, pages 221–231, 2019.
- [2] Alexander Alemi, Ben Poole, Ian Fischer, Joshua Dillon, Rif A Saurous, and Kevin Murphy. Fixing a broken elbow. In *International Conference on Machine Learning*, pages 159–168, 2018.
- [3] Martin Arjovsky, Soumith Chintala, and Léon Bottou. Wasserstein generative adversarial networks. In *International Conference on Machine Learning*, pages 214–223, 2017.
- [4] Yochai Blau and Tomer Michaeli. The perception-distortion tradeoff. In *Proceedings of the IEEE Conference on Computer Vision and Pattern Recognition*, pages 6228–6237, 2018.
- [5] Yochai Blau and Tomer Michaeli. Rethinking lossy compression: The rate-distortion-perception tradeoff. In *International Conference on Machine Learning*, pages 675–685, 2019.
- [6] Rob Breckelmanns, Daniel Moyer, Aram Galstyan, and Greg Ver Steeg. Exact rate-distortion in autoencoders via echo noise. In *Advances in Neural Information Processing Systems*, pages 3889–3900, 2019.
- [7] Thomas M Cover and Joy A Thomas. *Elements of information theory*. John Wiley & Sons, 1999.
- [8] DC Dowson and BV Landau. The fréchet distance between multivariate normal distributions. *Journal of multivariate analysis*, 12(3):450–455, 1982.
- [9] William HR Equitz and Thomas M Cover. Successive refinement of information. *IEEE Transactions on Information Theory*, 37(2):269–275, 1991.
- [10] Dror Freirich, Tomer Michaeli, and Ron Meir. A theory of the distortion-perception tradeoff in wasserstein space. *arXiv preprint arXiv:2107.02555*, 2021.
- [11] Ian Goodfellow, Jean Pouget-Abadie, Mehdi Mirza, Bing Xu, David Warde-Farley, Sherjil Ozair, Aaron Courville, and Yoshua Bengio. Generative adversarial nets. volume 27, pages 2672–2680, 2014.
- [12] Robert M Gray and Thomas G Stockham. Dithered quantizers. *IEEE Transactions on Information Theory*, 39(3):805–812, 1993.
- [13] Ishaan Gulrajani, Faruk Ahmed, Martin Arjovsky, Vincent Dumoulin, and Aaron C Courville. Improved training of wasserstein gans. In *Advances in neural information processing systems*, pages 5767–5777, 2017.
- [14] Martin Heusel, Hubert Ramsauer, Thomas Unterthiner, Bernhard Nessler, and Sepp Hochreiter. Gans trained by a two time-scale update rule converge to a local nash equilibrium. In *Advances in Neural Information Processing Systems*, pages 6626–6637, 2017.
- [15] Sicong Huang, Alireza Makhzani, Yanshuai Cao, and Roger Grosse. Evaluating lossy compression rates of deep generative models. In *International Conference on Machine Learning*, pages 4444–4454, 2020.
- [16] Justin Johnson, Alexandre Alahi, and Li Fei-Fei. Perceptual losses for real-time style transfer and super-resolution. In *European conference on computer vision*, pages 694–711. Springer, 2016.
- [17] Anders Boesen Lindbo Larsen, Søren Kaae Sønderby, Hugo Larochelle, and Ole Winther. Autoencoding beyond pixels using a learned similarity metric. In *International Conference on Machine Learning*, pages 1558–1566, 2016.
- [18] Luis Lastras and Toby Berger. All sources are nearly successively refinable. *IEEE Transactions on Information Theory*, 47(3):918–926, 2001.

- [19] Cheuk Ting Li and Abbas El Gamal. Strong functional representation lemma and applications to coding theorems. *IEEE Transactions on Information Theory*, 64(11):6967–6978, 2018.
- [20] Dong Liu, Haochen Zhang, and Zhiwei Xiong. On the classification-distortion-perception tradeoff. In *Advances in Neural Information Processing Systems*, pages 1206–1215, 2019.
- [21] Fabian Mentzer, Eirikur Agustsson, Michael Tschannen, Radu Timofte, and Luc Van Gool. Conditional probability models for deep image compression. In *Proceedings of the IEEE Conference on Computer Vision and Pattern Recognition*, pages 4394–4402, 2018.
- [22] Fabian Mentzer, George D Toderici, Michael Tschannen, and Eirikur Agustsson. High-fidelity generative image compression. In *Advances in Neural Information Processing Systems*, volume 33, 2020.
- [23] Anish Mittal, Anush K Moorthy, and Alan C Bovik. Blind/referenceless image spatial quality evaluator. In *2011 conference record of the forty fifth asilomar conference on signals, systems and computers (ASILOMAR)*, pages 723–727. IEEE, 2011.
- [24] Anish Mittal, Rajiv Soundararajan, and Alan C Bovik. Making a “completely blind” image quality analyzer. *IEEE Signal processing letters*, 20(3):209–212, 2012.
- [25] Youssef Mroueh, Tom Sercu, and Vaibhava Goel. Mcgan: Mean and covariance feature matching gan. In *International Conference on Machine Learning*, pages 2527–2535, 2017.
- [26] Sebastian Nowozin, Botond Cseke, and Ryota Tomioka. f-gan: training generative neural samplers using variational divergence minimization. In *Advances in Neural Information Processing Systems*, pages 271–279, 2016.
- [27] Naci Saldi, Tamás Linder, and Serdar Yüksel. Randomized quantization and optimal design with a marginal constraint. In *2013 IEEE International Symposium on Information Theory*, pages 2349–2353. IEEE, 2013.
- [28] Naci Saldi, Tamás Linder, and Serdar Yüksel. Output constrained lossy source coding with limited common randomness. *IEEE Transactions on Information Theory*, 61(9):4984–4998, 2015.
- [29] Leonard Schuchman. Dither signals and their effect on quantization noise. *IEEE Transactions on Communication Technology*, 12(4):162–165, 1964.
- [30] Lucas Theis and Eirikur Agustsson. On the advantages of stochastic encoders. *arXiv preprint arXiv:2102.09270*, 2021.
- [31] Lucas Theis and Aaron B Wagner. A coding theorem for the rate-distortion-perception function. *arXiv preprint arXiv:2104.13662*, 2021.
- [32] George Toderici, Damien Vincent, Nick Johnston, Sung Jin Hwang, David Minnen, Joel Shor, and Michele Covell. Full resolution image compression with recurrent neural networks. In *Proceedings of the IEEE Conference on Computer Vision and Pattern Recognition*, pages 5306–5314, 2017.
- [33] Michael Tschannen, Eirikur Agustsson, and Mario Lucic. Deep generative models for distribution-preserving lossy compression. In *Advances in Neural Information Processing Systems*, pages 5929–5940, 2018.
- [34] Michael Tschannen, Olivier Bachem, and Mario Lucic. Recent advances in autoencoder-based representation learning. *arXiv preprint arXiv:1812.05069*, 2018.
- [35] N Venkatanath, D Praneeth, Maruthi Chandrasekhar Bh, Sumohana S Channappayya, and Swarup S Medasani. Blind image quality evaluation using perception based features. In *2015 Twenty First National Conference on Communications (NCC)*, pages 1–6. IEEE, 2015.
- [36] Zhou Wang, Eero P Simoncelli, and Alan C Bovik. Multiscale structural similarity for image quality assessment. In *The Thrity-Seventh Asilomar Conference on Signals, Systems & Computers, 2003*, volume 2, pages 1398–1402. IEEE, 2003.

- [37] Zhou Wang, Alan C Bovik, Hamid R Sheikh, and Eero P Simoncelli. Image quality assessment: from error visibility to structural similarity. *IEEE transactions on image processing*, 13(4): 600–612, 2004.
- [38] Alan S. Willsky and Gregory W. Wornell. 6.432 lecture notes. <https://www.rle.mit.edu/sia/wp-content/uploads/2015/04/chapter3.pdf>, 2005.
- [39] Zeyu Yan, Fei Wen, Rendong Ying, Chao Ma, and Peilin Liu. On perceptual lossy compression: The cost of perceptual reconstruction and an optimal training framework. In *International Conference on Machine Learning*, 2021.
- [40] Ram Zamir and Kenneth Rose. Natural type selection in adaptive lossy compression. *IEEE Transactions on information theory*, 47(1):99–111, 2001.
- [41] Richard Zhang, Phillip Isola, Alexei A Efros, Eli Shechtman, and Oliver Wang. The unreasonable effectiveness of deep features as a perceptual metric. In *Proceedings of the IEEE conference on computer vision and pattern recognition*, pages 586–595, 2018.
- [42] Jacob Ziv. On universal quantization. *IEEE Transactions on Information Theory*, 31(3):344–347, 1985.

A Theoretical Results

A.1 Gaussian Case

Recall that for $X \sim \mathcal{N}(\mu_X, \sigma_X^2)$,

$$R(D) = \begin{cases} \frac{1}{2} \log(\sigma_X^2/D), & 0 \leq D \leq \sigma_X^2, \\ 0, & D > \sigma_X^2, \end{cases} \quad (15)$$

and in the first case the function is attained by some $p_{\hat{X}|X}$ with marginal $\hat{X} \sim \mathcal{N}(\mu_X, \sigma_X^2 - D)$ [7].

Theorem 1. For $X \sim \mathcal{N}(\mu_X, \sigma_X^2)$, the rate-distortion-perception function under squared error distortion and squared W_2 distance is achieved by some \hat{X} jointly Gaussian with X and is given by

$$R(D, P) = \begin{cases} \frac{1}{2} \log \frac{\sigma_X^2(\sigma_X - \sqrt{P})^2}{\sigma_X^2(\sigma_X - \sqrt{P})^2 - (\frac{\sigma_X^2 + (\sigma_X - \sqrt{P})^2 - D}{\sigma_X})^2} & \text{if } \sqrt{P} < \sigma_X - \sqrt{|\sigma_X^2 - D|}, \\ \max\{\frac{1}{2} \log \frac{\sigma_X^2}{D}, 0\} & \text{if } \sqrt{P} \geq \sigma_X - \sqrt{|\sigma_X^2 - D|}. \end{cases}$$

We will first need a Lemma from estimation theory. Let \hat{X} be a random variable with $\mathbb{E}[\hat{X}] = \mu_{\hat{X}}$, $\text{Var}(\hat{X}) = \sigma_{\hat{X}}^2$ and $\text{Cov}(X, \hat{X}) = \theta$. Let \hat{X}_G be a random variable jointly Gaussian with X with the same first and second order statistics as \hat{X} .

Lemma 1. Given $\mu_{\hat{X}}$, $\sigma_{\hat{X}}^2$, and θ , we have that

$$\mathbb{E}[(X - \mathbb{E}[X|\hat{X}_G])^2] \geq \mathbb{E}[(X - \mathbb{E}[X|\hat{X}])^2].$$

The proof of this result can be found in a standard estimation theory reference, e.g. Chapter 3, page 134 of the 6.432 notes by Willsky & Wornell [38].

Proof of Theorem 1. We shall show that there is no loss of optimality in assuming that \hat{X} is jointly Gaussian with X . It is clear that $\mathbb{E}[(X - \hat{X})^2] = \mathbb{E}[(X - \hat{X}_G)^2]$, as the first and second order statistics are all given. Note that by expanding out $W_2(p_X, p_{\hat{X}})$, one can see that the optimal coupling is identified only through the cross-term between X and \hat{X} ; since every coupling of p_X and $p_{\hat{X}}$ induces a Gaussian coupling of p_X and $p_{\hat{X}_G}$ with the same covariance, it follows that

$$W_2^2(p_X, p_{\hat{X}}) \geq W_2^2(p_X, p_{\hat{X}_G}). \quad (16)$$

Finally, we have

$$\begin{aligned} I(X; \hat{X}) &= h(X) - h(X|\hat{X}) \\ &\geq h(X) - h(X - \mathbb{E}[X|\hat{X}]) \\ &\stackrel{(a)}{\geq} h(X) - \frac{1}{2} \log(2\pi e \mathbb{E}[(X - \mathbb{E}[X|\hat{X}])^2]) \\ &\stackrel{(b)}{\geq} h(X) - \frac{1}{2} \log(2\pi e \mathbb{E}[(X - \mathbb{E}[X|\hat{X}_G])^2]) \\ &= h(X) - h(X - \mathbb{E}[X|\hat{X}_G]) \\ &\stackrel{(c)}{=} h(X) - h(X|\hat{X}_G) \\ &= I(X; \hat{X}_G), \end{aligned} \quad (17)$$

where (a) is because the Gaussian distribution maximizes differential entropy for a given variance, (b) follows from Lemma 1 and (c) is because the estimation error is independent of \hat{X}_G . Thus, it suffices to solve the problem

$$\begin{aligned} R(D, P) &= \min_{p_{\hat{X}_G|X}} I(X; \hat{X}_G) \\ \text{s.t. } &\mathbb{E}[(X - \hat{X}_G)^2] \leq D, \quad W_2^2(p_X, p_{\hat{X}_G}) \leq P. \end{aligned} \quad (18)$$

Note that we can write

$$\mathbb{E}[(X - \hat{X}_G)^2] = (\mu_X - \mu_{\hat{X}})^2 + \sigma_X^2 + \sigma_{\hat{X}}^2 - 2\theta, \quad (19)$$

and we have from standard results (e.g. minimizing (19), or more generally [8]) that

$$W_2^2(p_X, p_{\hat{X}_G}) = (\mu_X - \mu_{\hat{X}})^2 + (\sigma_X - \sigma_{\hat{X}})^2. \quad (20)$$

Finally, recall that the mutual information between the two Gaussian distributions is given by

$$I(X; \hat{X}_G) = \frac{1}{2} \log \frac{\sigma_X^2 \sigma_{\hat{X}}^2}{\sigma_X^2 \sigma_{\hat{X}}^2 - \theta^2}, \quad (21)$$

so there is no loss of optimality in assuming $\mu_{\hat{X}} = \mu_X$ and $\theta \geq 0$. Now we consider when each constraint is active. Suppose that P was active and D was inactive. Then

$$\begin{aligned} D &> \sigma_X^2 + \sigma_{\hat{X}}^2 - 2\theta \\ &= \sigma_X^2 + (\sigma_X - \sqrt{P})^2 - 2\theta. \end{aligned} \quad (22)$$

Hence, we can decrease θ to reduce the mutual information until either D is active or the rate is zero.

If D is active, then the perception constraint is satisfied automatically when $(\sigma_{\hat{X}} - \sigma_X)^2 \leq P$, or $\sqrt{P} \geq \sigma_X - \sqrt{|\sigma_X^2 - D|}$ (here we have used the solution to $R(D)$ from (15)). When $\sqrt{P} < \sigma_X - \sqrt{|\sigma_X^2 - D|}$, both P and D are active, and consequently we have $\sigma_{\hat{X}}^2 = (\sigma_X - \sqrt{P})^2$ and $\theta = \frac{\sigma_X^2 + \sigma_{\hat{X}}^2 - D}{2}$. Noting that the other case is simply the solution to $R(D)$, this concludes the proof. \square

Alternatively, we may express the minimum achievable distortion in terms of P and R as

$$D(P, R) = \begin{cases} \sigma_X^2 + (\sigma_X - \sqrt{P})^2 - 2\sigma_X(\sigma_X - \sqrt{P})\sqrt{1 - 2^{-2R}}, & P < (\sigma_X - \sqrt{\sigma_X^2 - \sigma_X^2 2^{-2R}})^2, \\ \sigma_X^2 2^{-2R}, & P \geq (\sigma_X - \sqrt{\sigma_X^2 - \sigma_X^2 2^{-2R}})^2. \end{cases}$$

For any fixed R , as P increases from 0 to $(\sigma_X - \sqrt{\sigma_X^2 - \sigma_X^2 2^{-2R}})^2$, $D(P, R)$ decreases from $2\sigma_X^2 - 2\sigma_X^2 \sqrt{1 - 2^{-2R}}$ to $\sigma_X^2 2^{-2R}$; further increasing P does not affect $D(P, R)$ anymore.

Moreover, the proof of Theorem 1 can be modified to handle to the case $d(p_X, p_{\hat{X}}) = \text{KL}(p_X, p_{\hat{X}})$, where $\text{KL}(p_X, p_{\hat{X}}) = \int p_{\hat{X}}(x) \log \frac{p_X(x)}{p_{\hat{X}}(x)} dx$ is the KL-divergence between p_X and $p_{\hat{X}}$. Given $(\mu_{\hat{X}}, \sigma_{\hat{X}}^2)$, $\text{KL}(p_X, p_{\hat{X}})$ is minimized when $p_{\hat{X}}$ is a Gaussian distribution. We have that

$$\begin{aligned} \text{KL}(p_X, p_{\hat{X}_G}) &= \frac{\sigma_{\hat{X}}^2 - \sigma_X^2}{2\sigma_X^2} + \frac{1}{2} \log \frac{\sigma_X^2}{\sigma_{\hat{X}}^2}, \\ W_2^2(p_X, p_{\hat{X}_G}) &= (\sigma_X - \sigma_{\hat{X}})^2. \end{aligned}$$

When $\sigma_{\hat{X}} \leq \sigma_X$, both functions are monotonically decreasing in $\sigma_{\hat{X}}$. This implies that the rate-distortion-perception functions under $\text{KL}(p_X, \cdot)$ and $W_2^2(p_X, \cdot)$ also share a one-to-one correspondence in P .

A.2 Achievability of Universal Representations

Before moving on to the achievability of universal representations, we first discuss the functional representations lemmas which play an integral part in the proof. The functional representation lemma states that for jointly distributed random variables X and Y , there exists a random variable U independent of X , and function ϕ such that $Y = \phi(X, U)$. Here, U is not necessarily unique. The strong functional representation lemma [19] states further that there exists a U which is informative of Y in the sense that

$$H(Y|U) \leq I(X; Y) + \log(I(X; Y) + 1) + 4.$$

Note that X and Y may be continuous random variables, and the entropy is still well-defined as long as $Y|U = u$ is discrete for each u . The construction given in [19] satisfies this property.

Theorem 2.

- (a) $R^*(\Theta) \leq R(\Theta) + \log(R(\Theta) + 1) + 5$.
(b) $R^*(\Theta) \geq R(\Theta)$.

Proof of Theorem 2. (a) Let Z be jointly distributed with X such that for any $(D, P) \in \Theta$, there exists $p_{\hat{X}_{D,P}|Z}$ satisfying $\mathbb{E}[\Delta(X, \hat{X}_{D,P})] \leq D$ and $d(p_X, p_{\hat{X}_{D,P}}) \leq P$. It follows by the strong functional representation lemma that there exist a random variable V , independent of X , and a deterministic function ϕ such that $Z = \phi(X, V)$ and $H(\phi(X, V)|V) \leq I(X; Z) + \log(I(X; Z) + 1) + 4$. So with V available at both the encoder and the decoder, we can use a class of prefix-free binary codes indexed by V with the expected codeword length no greater than $I(X; Z) + \log(I(X; Z) + 1) + 5$ to lossless represent Z . Now it suffices for the decoder to simulate $p_{\hat{X}_{D,P}|Z}$. Specifically, it follows by the functional representation lemma that there exists a random variable $V_{D,P}$, independent of (X, V) , and a deterministic function $\psi_{D,P}$ such that $\hat{X}_{D,P} = \psi_{D,P}(Z, V_{D,P})$. Note that V and $V_{D,P}$ can be extracted from random seed U .

(b) For any random variable U , encoding function $f_U : \mathcal{X} \rightarrow \mathcal{C}_U$, and decoding functions $g_{U,D,P} : \mathcal{C}_U \rightarrow \hat{\mathcal{X}}$, $(D, P) \in \Theta$ satisfying $\mathbb{E}[\Delta(X, \hat{X}_{D,P})] \leq D$ and $d(p_X, p_{\hat{X}_{D,P}}) \leq P$, we have

$$\begin{aligned} \mathbb{E}[\ell(f_U(X))] &\geq H(f_U(X)|U) \\ &= I(X; f_U(X)|U) \\ &= I(X; f_U(X), U) \\ &\geq R(\Theta), \end{aligned}$$

where the last inequality follows by defining $(f_U(X), U)$ as Z , which satisfies the conditions in the definition of $R(\Theta)$. \square

Theorem 3. Let $X \sim \mathcal{N}(\mu_X, \sigma_X^2)$ be a scalar Gaussian source and assume MSE and $W_2^2(\cdot, \cdot)$ losses. Let Θ be any non-empty set of (D, P) pairs. Then

$$A(\Theta) = 0. \quad (23)$$

Moreover, for any representation Z jointly Gaussian with X such that

$$I(X; Z) = \sup_{(D,P) \in \Theta} R(D, P), \quad (24)$$

we have

$$\Theta \subseteq \Omega(p_{Z|X}) = \Omega(I(X; Z)). \quad (25)$$

Proof of Theorem 3. Let $R = \sup_{(D,P) \in \Theta} R(D, P)$. It is clear that $\Theta \subseteq \Omega(R)$. The distortion-perception tradeoff with respect to R , i.e., the lower boundary of $\Omega(R)$, is given by

$$D = \sigma_X^2 + (\sigma_X - \sqrt{P})^2 - 2\sigma_X(\sigma_X - \sqrt{P})\sqrt{1 - 2^{-2R}}, \quad P \in [0, (\sigma_X - \sqrt{\sigma_X^2 - \sigma_X^2 2^{-2R}})^2].$$

Every point in $\Omega(R)$ is dominated in a component-wise manner by some (D, P) on this tradeoff. Let Z be jointly Gaussian with X such that $I(X; Z) = R$. Note that $I(X; Z) = R$ implies $\rho_{XZ}^2 = 1 - 2^{-2R}$, where $\rho_{XZ} = \frac{\mathbb{E}[(X - \mu_X)(Z - \mu_Z)]}{\sigma_X \sigma_Z}$. For any (D, P) on the tradeoff, define $\hat{X}_{D,P} = \text{sign}(\rho_{XZ}) \frac{\sigma_X - \sqrt{P}}{\sigma_Z} (Z - \mu_Z) + \mu_X$, where $\text{sign}(\rho_{XZ}) = 1$ if $\rho_{XZ} \geq 0$ and $\text{sign}(\rho_{XZ}) = -1$ otherwise. One may verify by direct substitution that

$$\begin{aligned} W_2^2(p_X, p_{\hat{X}_{D,P}}) &= (\sigma_X - \sigma_{\hat{X}_{D,P}})^2 = P, \\ \mathbb{E}[(X - \hat{X}_{D,P})^2] &= \sigma_X^2 + \sigma_{\hat{X}_{D,P}}^2 - 2\sigma_X(\sigma_X - \sqrt{P})|\rho_{XZ}| \\ &= \sigma_X^2 + (\sigma_X - \sqrt{P})^2 - 2\sigma_X(\sigma_X - \sqrt{P})\sqrt{1 - 2^{-2R}} \\ &= D. \end{aligned}$$

This shows that $\Omega(p_{Z|X}) = \Omega(R)$, which further implies $A(\Theta) = 0$. \square

Proposition 1 (Equivalence of zero rate penalty and full distortion-perception region). Suppose the following regularity conditions hold:

- 1) $\sup_{(D,P) \in \Omega(R)} R(D, P) = R'$,
- 2) the infimum in the definition of $R(\Omega(R'))$ is attainable.

Then the equality $A(\Omega(R')) = 0$ holds if and only if there exists some representation Z with $I(X; Z) = R'$ such that $\Omega(p_{Z|X}) = \Omega(I(X; Z))$.

Proof of Proposition 1. If there exists some representation Z with $I(X; Z) = R'$ such that $\Omega(p_{Z|X}) = \Omega(I(X; Z))$, then $R(\Omega(R')) \leq R'$. Now under condition 1), we must have $A(\Omega(R')) \leq 0$, which implies $A(\Omega(R')) = 0$ as $A(\Omega(R'))$ must be nonnegative.

Under condition 2), there exists some representation Z with $I(X; Z) = R(\Omega(R'))$ such that $\Omega(p_{Z|X}) \supseteq \Omega(R')$. If $A(\Omega(R')) = 0$, then $R(\Omega(R')) = \sup_{(D,P) \in \Omega(R)} R(D, P)$, which together with condition 1) yields $R(\Omega(R')) = R$. Note that $I(X; Z) = R'$ implies $\Omega(p_{Z|X}) \subseteq \Omega(R')$, and consequently we must have $\Omega(p_{Z|X}) = \Omega(R')$. \square

Theorem 4. Assume MSE loss and any perception measure $d(\cdot, \cdot)$. Let Z be any arbitrary representation of X . Then

$$\Omega(p_{Z|X}) \subseteq \left\{ (D, P) : D \geq \mathbb{E}[\|X - \tilde{X}\|^2] + \inf_{p_{\tilde{X}}: d(p_X, p_{\tilde{X}}) \leq P} W_2^2(p_{\tilde{X}}, p_{\tilde{X}}) \right\} \subseteq \text{cl}(\Omega(p_{Z|X})),$$

where $\tilde{X} = \mathbb{E}[X|Z]$ is the reconstruction minimizing squared error distortion with X under the representation Z and $\text{cl}(\cdot)$ denotes set closure. In particular, the two extreme points $(D^{(a)}, P^{(a)}) = (\mathbb{E}[\|X - \tilde{X}\|^2], d(p_X, p_{\tilde{X}}))$ and $(D^{(b)}, P^{(b)}) = (\mathbb{E}[\|X - \tilde{X}\|^2] + W_2^2(p_{\tilde{X}}, p_X), 0)$ are contained in $\text{cl}(\Omega(p_{Z|X}))$.

Proof of Theorem 4. For any $(D, P) \in \Omega(p_{Z|X})$, there exists some $\hat{X}_{D,P}$ jointly distributed with (X, Z) such that $X \leftrightarrow Z \leftrightarrow \hat{X}_{D,P}$ form a Markov chain, $\mathbb{E}[\Delta(X, \hat{X}_{D,P})] \leq D$, and $d(p_X, p_{\hat{X}_{D,P}}) \leq P$. Note that

$$\begin{aligned} D &\geq \mathbb{E}[\|X - \hat{X}_{D,P}\|^2] \\ &= \mathbb{E}[\|X - \tilde{X}\|^2] + \mathbb{E}[\|\tilde{X} - \hat{X}_{D,P}\|^2] \\ &\geq \mathbb{E}[\|X - \tilde{X}\|^2] + W_2^2(p_{\tilde{X}}, p_{\hat{X}_{D,P}}) \\ &\geq \mathbb{E}[\|X - \tilde{X}\|^2] + \inf_{p_{\tilde{X}}: d(p_X, p_{\tilde{X}}) \leq P} W_2^2(p_{\tilde{X}}, p_{\tilde{X}}). \end{aligned}$$

Therefore, we have $\Omega(p_{Z|X}) \subseteq \{(D, P) : D \geq \mathbb{E}[\|X - \tilde{X}\|^2] + \inf_{p_{\tilde{X}}: d(p_X, p_{\tilde{X}}) \leq P} W_2^2(p_{\tilde{X}}, p_{\tilde{X}})\}$.

On the other hand, given

$$(D', P') \in \{(D, P) : D \geq \mathbb{E}[\|X - \tilde{X}\|^2] + \inf_{p_{\tilde{X}}: d(p_X, p_{\tilde{X}}) \leq P} W_2^2(p_{\tilde{X}}, p_{\tilde{X}})\},$$

for any $\epsilon > 0$, we can find some $p_{\hat{X}'}$ such that $d(p_X, p_{\hat{X}'}) \leq P'$ and $D' + \epsilon \geq \mathbb{E}[\|X - \tilde{X}\|^2] + W_2^2(p_{\tilde{X}}, p_{\hat{X}'})$. Let \hat{X}' be jointly distributed with (X, Z) such that $X \leftrightarrow Z \leftrightarrow \hat{X}'$ form a Markov chain and $\mathbb{E}[\|\tilde{X} - \hat{X}'\|^2] \leq W_2^2(p_{\tilde{X}}, p_{\hat{X}'}) + \epsilon$. It is possible to find such \hat{X}' by the Markov condition. Note that

$$\begin{aligned} \mathbb{E}[\|X - \hat{X}'\|^2] &= \mathbb{E}[\|X - \tilde{X}\|^2] + \mathbb{E}[\|\tilde{X} - \hat{X}'\|^2] \\ &\leq \mathbb{E}[\|X - \tilde{X}\|^2] + W_2^2(p_{\tilde{X}}, p_{\hat{X}'}) + \epsilon \\ &\leq D' + 2\epsilon. \end{aligned}$$

Therefore, we have

$$\{(D, P) : D \geq \mathbb{E}[\|X - \tilde{X}\|^2] + \inf_{p_{\tilde{X}}: d(p_X, p_{\tilde{X}}) \leq P} W_2^2(p_{\tilde{X}}, p_{\tilde{X}})\} \subseteq \text{cl}(\Omega(p_{Z|X})).$$

Choosing $p_{\hat{X}} = p_{\tilde{X}}$ and $p_{\hat{X}} = p_X$ shows respectively that $(D^{(a)}, P^{(a)})$ and $(D^{(b)}, P^{(b)})$ are contained in $\{(D, P) : D \geq \mathbb{E}[\|X - \tilde{X}\|^2] + \inf_{p_{\tilde{X}}: d(p_X, p_{\tilde{X}}) \leq P} W_2^2(p_{\tilde{X}}, p_X)\}$. \square

Quantitative results for the additive and multiplicative gaps. Since $P_3 = 0$ (i.e., $p_{\hat{X}_{D_3, P_3}} = p_X$), it follows that

$$D_3 = \mathbb{E}[\|X - \hat{X}_{D_3, P_3}\|^2] = 2\sigma_X^2 - 2\mathbb{E}[(X - \mu_X)^T(\hat{X}_{D_3, P_3} - \mu_X)]. \quad (26)$$

Note that $I(X; \mathbb{E}[X|\hat{X}_{D_3, P_3}]) \leq I(X; \hat{X}_{D_3, P_3}) = R(D_1, \infty)$, which implies $\mathbb{E}[\|X - \mathbb{E}[X|\hat{X}_{D_3, P_3}]\|^2] \geq D_1$. Let $c = \frac{2\sigma_X^2 - D_3}{2\sigma_X^2}$. We have

$$\begin{aligned} D_1 &\leq \mathbb{E}[\|X - \mathbb{E}[X|\hat{X}_{D_3, P_3}]\|^2] \\ &\leq \mathbb{E}[\|X - \mu_X - c(\hat{X}_{D_3, P_3} - \mu_X)\|^2] \\ &= (1 + c^2)\sigma_X^2 - 2c\mathbb{E}[(X - \mu_X)^T(\hat{X}_{D_3, P_3} - \mu_X)] \\ &\stackrel{(a)}{=} \frac{4\sigma_X^2 D_3 - D_3^2}{4\sigma_X^2}, \end{aligned}$$

where (a) is due to (26). So

$$D_3 \geq 2\sigma_X^2 - 2\sigma_X \sqrt{\sigma_X^2 - D_1},$$

which together with the fact that $D^{(b)} \leq 2D_1$ implies

$$\begin{aligned} D^{(b)} - D_3 &\leq 2D_1 - 2\sigma_X^2 + 2\sigma_X \sqrt{\sigma_X^2 - D_1}, \\ \frac{D^{(b)}}{D_3} &\leq \frac{D_1}{\sigma_X^2 - \sigma_X \sqrt{\sigma_X^2 - D_1}}. \end{aligned}$$

It is easy to verify that

$$\begin{aligned} \frac{1}{2}\sigma_X^2 &\geq 2D_1 - 2\sigma_X^2 + 2\sigma_X \sqrt{\sigma_X^2 - D_1} \stackrel{D_1 \approx 0 \text{ or } \sigma_X^2}{\approx} 0, \\ 2 &\geq \frac{D_1}{\sigma_X^2 - \sigma_X \sqrt{\sigma_X^2 - D_1}} \stackrel{D_1 \approx \sigma_X^2}{\approx} 1. \end{aligned}$$

A similar argument can be used to bound the gap between (D_1, P_1) and the upper-left extreme point $(\tilde{D}^{(a)}, \tilde{P}^{(a)})$ of blue curve. Note that

$$\tilde{D}^{(a)} = \mathbb{E}[\|X - \mathbb{E}[X|\hat{X}_{D_3, P_3}]\|^2] \leq \frac{4\sigma_X^2 D_3 - D_3^2}{4\sigma_X^2},$$

which together with the fact that $D_1 \geq \frac{1}{2}D_3$ implies

$$\begin{aligned} \tilde{D}^{(a)} - D_1 &\leq \frac{1}{2}D_3 - \frac{D_3^2}{4\sigma_X^2}, \\ \frac{\tilde{D}^{(a)}}{D_1} &\leq 2 - \frac{D_3}{2\sigma_X^2}. \end{aligned}$$

Finally, this implies

$$\frac{1}{4}\sigma_X^2 \geq \frac{1}{2}D_3 - \frac{D_3^2}{4\sigma_X^2} \stackrel{D_3 \approx 0 \text{ or } 2\sigma_X^2}{\approx} 0, \quad (27)$$

$$2 \geq 2 - \frac{D_3}{2\sigma_X^2} \stackrel{D_3 \approx 2\sigma_X^2}{\approx} 1. \quad (28)$$

We have previously dealt with the one-shot setting. Now we consider the case where we jointly encode an i.i.d. sequence X^n where each symbol has marginal distribution p_X . Here we assume that $d(\cdot, \cdot)$ is convex in its second argument.

Definition 4. Let Θ be an arbitrary set of (D, P) pairs. A Θ -universal representation of asymptotic rate R is said to exist if we can find a sequence of random variables $U^{(n)}$, encoding functions $f_{U^{(n)}}^{(n)} : \mathcal{X}^n \rightarrow \mathcal{C}_{U^{(n)}}^{(n)}$ and decoding functions $g_{U^{(n)}, D, P}^{(n)} : \mathcal{C}_{U^{(n)}}^{(n)} \rightarrow \hat{\mathcal{X}}^n$, $(D, P) \in \Theta$, satisfying

$$\frac{1}{n} \sum_{i=1}^n \mathbb{E}[\Delta(X(i), \hat{X}_{D, P}(i))] \leq D, \quad (29)$$

$$d\left(p_X, \frac{1}{n} \sum_{i=1}^n p_{\hat{X}_{D, P}(i)}\right) \leq P \quad (30)$$

such that

$$\limsup_{n \rightarrow \infty} \frac{1}{n} \mathbb{E}[\ell(f_{U^{(n)}}^{(n)}(X^n))] \leq R,$$

where $\hat{X}_{D, P}^n \triangleq g_{U^{(n)}, D, P}^{(n)}(f_{U^{(n)}}^{(n)}(X^n))$. The minimum of such R with respect to Θ is denoted as $R^{(\infty)}(\Theta)$.

Theorem 5. $R^{(\infty)}(\Theta) = R(\Theta)$.

Remark 1. The same conclusion holds if constraint (29) is replaced with

$$\mathbb{E}[\Delta(X(i), \hat{X}_{D, P}(i))] \leq D, \quad i = 1, \dots, n, \quad (31)$$

and/or constraint (30) is replaced with

$$d(p_X, p_{\hat{X}_{D, P}(i)}) \leq P, \quad i = 1, \dots, n. \quad (32)$$

Note that (31) and (32) are more relaxed than (29) and (30), respectively, as

$$(31) \Rightarrow (29),$$

$$(32) \Rightarrow \frac{1}{n} \sum_{i=1}^n d(p_X, p_{\hat{X}_{D, P}(i)}) \Rightarrow (30).$$

Moreover, it is easy to verify that under constraints (31) and (32), Theorem 5 holds without the convexity assumption on $d(\cdot, \cdot)$.

Proof of Theorem 5. Let Z be jointly distributed with X such that for any $(D, P) \in \Theta$, there exists $p_{\hat{X}_{D, P}|Z}$ satisfying $\mathbb{E}[\Delta(X, \hat{X}_{D, P})] \leq D$ and $d(p_X, p_{\hat{X}_{D, P}}) \leq P$. Construct

$$p_{Z^n|X^n} \triangleq \prod_{i=1}^n p_{Z(i)|X(i)}$$

with $p_{Z(i)|X(i)} = p_{Z|X}$, $i = 1, \dots, n$. It follows by the strong functional representation lemma that there exists a random variable $V^{(n)}$, independent of X^n , and a deterministic function $\phi^{(n)}$ such that $Z^n = \phi(X^n, V^{(n)})$ and $H(\phi(X^n, V^{(n)})|V^{(n)}) \leq I(X^n; Z^n) + \log(I(X^n; Z^n) + 1) + 4$. So with $V^{(n)}$ available at both the encoder and the decoder, we can use a class of prefix-free binary codes indexed by $V^{(n)}$ with the expected codeword length no greater than $I(X^n; Z^n) + \log(I(X^n; Z^n) + 1) + 5$ to lossless represent Z^n . Moreover, by the functional representation lemma, there exist a random variable $V_{D, P}$, independent of $(X^n; V^{(n)})$, and a deterministic function $\psi_{D, P}$ such that $p_{\psi_{D, P}(Z(i), V_{D, P})|Z(i)} = p_{\hat{X}_{D, P}|Z}$. Note that $V^{(n)}$ and $V_{D, P}$ can be extracted from random seed $U^{(n)}$. Define $\hat{X}_{D, P}(i) = \psi_{D, P}(Z(i), V_{D, P})$, $i = 1, \dots, n$. It is easy to verify that

$$\frac{1}{n} \sum_{i=1}^n \mathbb{E}[\Delta(X(i), \hat{X}_{D, P}(i))] = \mathbb{E}[\Delta(X, \hat{X}_{D, P})] \leq D,$$

$$d\left(p_X, \frac{1}{n} \sum_{i=1}^n p_{\hat{X}_{D, P}(i)}\right) = d(p_X, p_{\hat{X}_{D, P}}) \leq P.$$

Moreover, notice that

$$\begin{aligned} & \frac{1}{n}I(X^n; Z^n) + \frac{1}{n} \log(I(X^n; Z^n) + 1) + \frac{5}{n} \\ &= I(X; Z) + \frac{1}{n} \log(nI(X; Z) + 1) + \frac{5}{n} \\ & \xrightarrow{n \rightarrow \infty} I(X; Z). \end{aligned}$$

This proves that $R^{(\infty)}(\Theta) \leq R(\Theta)$.

For any random variable $U^{(n)}$, encoding function $f_{U^{(n)}}^{(n)} : \mathcal{X}^n \rightarrow \mathcal{C}_{U^{(n)}}^{(n)}$ and decoding function $g_{U^{(n)}, D, P}^{(n)} : \mathcal{C}_{U^{(n)}}^{(n)} \rightarrow \hat{\mathcal{X}}^n$, $(D, P) \in \Theta$ satisfying (29) and (30), we have

$$\begin{aligned} \frac{1}{n} \mathbb{E}[\ell(f_{U^{(n)}}^{(n)}(X^n))] &\geq \frac{1}{n} H(f_{U^{(n)}}^{(n)}(X^n) | U^{(n)}) \\ &= \frac{1}{n} I(X^n; f_{U^{(n)}}^{(n)}(X^n) | U^{(n)}) \\ &= \frac{1}{n} \sum_{i=1}^n I(X(i); f_{U^{(n)}}^{(n)}(X^n) | U^{(n)}, X^{i-1}) \\ &= \frac{1}{n} \sum_{i=1}^n I(X(i); f_{U^{(n)}}^{(n)}(X^n), U^{(n)}, X^{i-1}) \\ &\geq \frac{1}{n} \sum_{i=1}^n I(X(i); f_{U^{(n)}}^{(n)}(X^n), U^{(n)}) \\ &= I(X(T); f_{U^{(n)}}^{(n)}(X^n), U^{(n)} | T) \\ &= I(X(T); f_{U^{(n)}}^{(n)}(X^n), U^{(n)}, T), \end{aligned}$$

where T is uniformly distributed over $\{1, \dots, n\}$ and is independent of X^n and $U^{(n)}$. Note that $\hat{X}_{D, P}(T)$ is a function of $(f_{U^{(n)}}^{(n)}(X^n), U^{(n)}, T)$ for any $(D, P) \in \Theta$. Since

$$\begin{aligned} p_{X(T)} &= p_X, \\ \mathbb{E}[\Delta(X(T), \hat{X}_{D, P}(T))] &= \frac{1}{n} \sum_{i=1}^n \mathbb{E}[\Delta(X(i), \hat{X}_{D, P}(i))] \leq D, \\ d(p_{X(T)}, p_{\hat{X}_{D, P}(T)}) &= d\left(p_X, \frac{1}{n} \sum_{i=1}^n p_{\hat{X}_{D, P}(i)}\right) \leq P, \end{aligned}$$

it follows that

$$I(X(T); f_{U^{(n)}}^{(n)}(X^n), U, T) \geq R(\Theta).$$

This completes the proof. \square

A.3 Successive Refinement

We now study the case where the rate is not fixed in advance. Bits are sent in two stages as opposed to all at once, with the hope that the reconstructions produced at both stages perform near-optimally in both perception and distortion compared to what can be achieved by one-stage communication at both the lower rate and the higher rate. Two-stage procedures arise frequently under practical constraints, and previous works have considered this only under distortion losses. We address the extension of universal representations to this setting within the successive refinement [9] framework.

Definition 5 (Two-stage Coding). Given two sets of (D, P) pairs Θ_1 and Θ_2 , we say rate pair (R_1, R_2) is (operationally) achievable if there exists random variable U , encoding functions

$$f_U : \mathcal{X} \rightarrow \mathcal{C}_U, \quad f_{U, f_U(X)} : \mathcal{X} \rightarrow \mathcal{C}_{U, f_U(X)},$$

and decoding functions

$$g_{U,D_1,P_1} : \mathcal{C}_U \rightarrow \hat{\mathcal{X}}, \quad g_{U,f_U(X),D_2,P_2} : \mathcal{C}_{U,f_U(X)} \rightarrow \hat{\mathcal{X}}$$

for each $(D_1, P_1) \in \Theta_1$ and $(D_2, P_2) \in \Theta_2$, such that

$$\begin{aligned} \mathbb{E}[\ell(f_U(X))] &\leq R_1, & \mathbb{E}[\ell(f_{U,f_U(X)}(X))] &\leq R_2, \\ \mathbb{E}[\Delta(X, \hat{X}_{1,D_1,P_1})] &\leq D_1, & \mathbb{E}[\Delta(X, \hat{X}_{2,D_2,P_2})] &\leq D_2, \\ d(p_X, p_{\hat{X}_{1,D_1,P_1}}) &\leq P_1, & d(p_X, p_{\hat{X}_{2,D_2,P_2}}) &\leq P_2, \end{aligned}$$

where $\hat{X}_{1,D_1,P_1} = g_{U,D_1,P_1}(f_U(X))$ and $\hat{X}_{2,D_2,P_2} = g_{U,f_U(X),D_2,P_2}(f_{U,f_U(X)}(X))$. The closure of the set of such (R_1, R_2) is denoted as $\mathcal{R}^*(\Theta_1, \Theta_2)$.

Here, f_U acts with each g_{U,D_1,P_1} forming a low rate encoder-decoder pair to meet each constraint $(D_1, P_1) \in \Theta_1$. Thereafter, $f_{U,f_U(X)}$ encodes additional information about the source which is combined with the low rate encoding to produce a high rate reconstruction through $g_{U,f_U(X),D_2,P_2}$ meeting each constraint $(D_2, P_2) \in \Theta_2$.

Definition 6 (Inner and outer bounds). Define

$$\begin{aligned} \underline{\mathcal{R}}(\Theta_1, \Theta_2) &= \bigcup_{p_{Z_1, Z_2|X}} \{(R_1, R_2) \in \mathbb{R}_+^2 : R_1 \geq I(X; Z_1) + \log(I(X; Z_1) + 1) + 5, \\ &\quad R_1 + R_2 \geq I(X; Z_1, Z_2) + \log(I(X; Z_1) + 1) + \log(I(X; Z_2|Z_1) + 1) + 10\}, \\ \overline{\mathcal{R}}(\Theta_1, \Theta_2) &= \bigcup_{p_{Z_1, Z_2|X}} \{(R_1, R_2) \in \mathbb{R}_+^2 : R_1 \geq I(X; Z_1), R_1 + R_2 \geq I(X; Z_1, Z_2)\} \end{aligned}$$

with the unions taken over $p_{Z_1, Z_2|X}$ such that for any $(D_1, P_1) \in \Theta_1$ and $(D_2, P_2) \in \Theta_2$, there exists

$$p_{\hat{X}_{1,D_1,P_1}|Z_1} \quad \text{and} \quad p_{\hat{X}_{2,D_2,P_2}|Z_2}$$

satisfying

$$\begin{aligned} \mathbb{E}[\Delta(X, \hat{X}_{1,D_1,P_1})] &\leq D_1, & \mathbb{E}[\Delta(X, \hat{X}_{2,D_2,P_2})] &\leq D_2, \\ d(p_X, p_{\hat{X}_{1,D_1,P_1}}) &\leq P_1, & d(p_X, p_{\hat{X}_{2,D_2,P_2}}) &\leq P_2. \end{aligned}$$

We now characterize the operational definition in terms of these information rate regions.

Theorem 6. $cl(\underline{\mathcal{R}}(\Theta_1, \Theta_2)) \subseteq \mathcal{R}^*(\Theta_1, \Theta_2) \subseteq cl(\overline{\mathcal{R}}(\Theta_1, \Theta_2))$.

Proof of Theorem 6. (a) Let Z_1 and Z_2 be jointly distributed with X such that for any $(D_1, P_1) \in \Theta_1$ and $(D_2, P_2) \in \Theta_2$, there exist $p_{\hat{X}_{1,D_1,P_1}|Z_1}$ and $p_{\hat{X}_{2,D_2,P_2}|Z_2}$ satisfying $\mathbb{E}[\Delta(X, \hat{X}_{1,D_1,P_1})] \leq D_1$, $\mathbb{E}[\Delta(X, \hat{X}_{2,D_2,P_2})] \leq D_2$, $d(p_X, p_{\hat{X}_{1,D_1,P_1}}) \leq P_1$, and $d(p_X, p_{\hat{X}_{2,D_2,P_2}}) \leq P_2$. It follows by the strong functional representation lemma that there exist a random variable V_1 , independent of X , and a deterministic function ϕ_1 such that $Z_1 = \phi_1(X, V_1)$ and $H(\phi_1(X, V_1)|V_1) \leq I(X; Z_1) + \log(I(X; Z_1) + 1) + 4$; moreover, there exist a random variable V_2 , independent of (X, V_1) , and a deterministic function ϕ_2 such that $Z_2 = \phi_2(X, Z_1, V_2)$ and $H(\phi_2(X, Z_1, V_2)|Z_1, V_2) \leq I(X; Z_2|Z_1) + \log(I(X; Z_2|Z_1) + 1) + 4$. So with (V_1, V_2) available at both the encoder and the decoder, we can use a class of prefix-free binary codes indexed by V_1 with the expected codeword length no greater than $I(X; Z_1) + \log(I(X; Z_1) + 1) + 5$ to lossless represent Z_1 and then use a class of prefix-free binary codes indexed by (Z_1, V_2) with the expected codeword length no greater than $I(X; Z_2|Z_1) + \log(I(X; Z_2|Z_1) + 1) + 5$ to lossless represent Z_2 . Note that in the first stage we can send the codeword used to represent Z_1 and with a certain probability the codeword used to represent Z_2 .

Now it suffices for the decoder to simulate $p_{\hat{X}_{1,D_1,P_1}|Z_1}$ and $p_{\hat{X}_{2,D_2,P_2}|Z_2}$. Specifically, it follows by the functional representation lemma that there exist random variables

$$V_{1,D_1,P_1} \quad \text{and} \quad V_{2,D_2,P_2},$$

independent of (X, V_1, V_2) , and deterministic functions

$$\psi_{1,D_1,P_1} \quad \text{and} \quad \psi_{2,D_2,P_2}$$

such that

$$\begin{aligned} \hat{X}_{1,D_1,P_1} &= \psi_{1,D_1,P_1}(Z_1, V_{1,D_1,P_1}), \\ \hat{X}_{2,D_2,P_2} &= \psi_{2,D_2,P_2}(Z_2, V_{2,D_2,P_2}). \end{aligned}$$

This proves the desired result.

(b) For any random variable U , encoding functions $f_U : \mathcal{X} \rightarrow \mathcal{C}_U$, $f_{U,f_U(X)} : \mathcal{X} \rightarrow \mathcal{C}_{U,f_U(X)}$ and decoding functions $g_{U,D_1,P_1} : \mathcal{C}_U \rightarrow \hat{\mathcal{X}}$, $(D_1, P_1) \in \Theta_1$, $g_{U,f_U(X),D_2,P_2} : \mathcal{C}_{U,f_U(X)} \rightarrow \hat{\mathcal{X}}$, $(D_2, P_2) \in \Theta_2$, satisfying $\mathbb{E}[\Delta(X, \hat{X}_{1,D_1,P_1})] \leq D_1$, $\mathbb{E}[\Delta(X, \hat{X}_{2,D_2,P_2})] \leq D_2$, $d(p_X, p_{\hat{X}_{1,D_1,P_1}}) \leq P_1$, and $d(p_X, p_{\hat{X}_{2,D_2,P_2}}) \leq P_2$, we have

$$\begin{aligned} \mathbb{E}[\ell(f_U(X))] &\geq H(f_U(X)|U) \\ &= I(X; f_U(X)|U) \\ &\geq I(X; f_U(X), U) \\ &= I(X; Z_1) \end{aligned}$$

and

$$\begin{aligned} \mathbb{E}[\ell(f_U(X))] + \mathbb{E}[\ell(f_{U,f_U(X)}(X))] &\geq H(f_U(X)|U) + H(f_{U,f_U(X)}(X)|U, f_U(X)) \\ &\geq I(X; f_U(X)|U) + I(X; f_{U,f_U(X)}(X)|U, f_U(X)) \\ &= I(X; f_U(X), f_{U,f_U(X)}(X)|U) \\ &= I(X; f_U(X), f_{U,f_U(X)}(X), U) \\ &= I(X; Z_1, Z_2), \end{aligned}$$

where we define $Z_1 = (f_U(X), U)$ and $Z_2 = (f_U(X), f_{U,f_U(X)}(X), U)$. So $(R_1, R_2) \in \overline{\mathcal{R}}(\Theta_1, \Theta_2)$ for any (R_1, R_2) with $R_1 \geq \mathbb{E}[\ell(f_U(X))]$ and $R_2 \geq \mathbb{E}[\ell(f_{U,f_U(X)}(X))]$. This completes the proof. \square

Definition 7 (Asymptotic rate region). Given two sets of (D, P) pairs Θ_1 and Θ_2 , we say rate pair (R_1, R_2) is asymptotically achievable if there exists a sequence of random variables $U^{(n)}$, encoding functions

$$f_{U^{(n)}}^{(n)} : \mathcal{X}^n \rightarrow \mathcal{C}_{U^{(n)}}^{(n)}, \quad f_{U^{(n)}, f_{U^{(n)}}^{(n)}(X^n)}^{(n)} : \mathcal{X}^n \rightarrow \mathcal{C}_{U^{(n)}, f_{U^{(n)}}^{(n)}(X^n)}^{(n)}$$

and decoding functions

$$g_{U^{(n)}, D_1, P_1}^{(n)} : \mathcal{C}_{U^{(n)}}^{(n)} \rightarrow \hat{\mathcal{X}}^n, \quad g_{U^{(n)}, f_{U^{(n)}}^{(n)}(X^n), D_2, P_2}^{(n)} : \mathcal{C}_{U^{(n)}, f_{U^{(n)}}^{(n)}(X^n)}^{(n)} \rightarrow \hat{\mathcal{X}}^n$$

$(D_1, P_1) \in \Theta_1$, $(D_2, P_2) \in \Theta_2$, satisfying

$$\frac{1}{n} \sum_{i=1}^n \mathbb{E}[\Delta(X(i), \hat{X}_{1,D_1,P_1}(i))] \leq D_1, \quad \frac{1}{n} \sum_{i=1}^n \mathbb{E}[\Delta(X(i), \hat{X}_{2,D_2,P_2}(i))] \leq D_2, \quad (33)$$

$$d\left(p_X, \frac{1}{n} \sum_{i=1}^n p_{\hat{X}_{1,D_1,P_1}(i)}\right) \leq P_1, \quad d\left(p_X, \frac{1}{n} \sum_{i=1}^n p_{\hat{X}_{2,D_2,P_2}(i)}\right) \leq P_2 \quad (34)$$

such that

$$\limsup_{n \rightarrow \infty} \frac{1}{n} \mathbb{E}[\ell(f_{U^{(n)}}^{(n)}(X^n))] \leq R_1, \quad \limsup_{n \rightarrow \infty} \frac{1}{n} \mathbb{E}[\ell(f_{U^{(n)}, f_{U^{(n)}}^{(n)}(X^n)}^{(n)}(X^n))] \leq R_2,$$

where

$$\hat{X}_{1,D_1,P_1}^n = g_{U^{(n)}, D_1, P_1}^{(n)}(f_{U^{(n)}}^{(n)}(X^n))$$

and

$$\hat{X}_{2,D_2,P_2}^n = g_{U^{(n)}, f_{U^{(n)}}^{(n)}(X^n), D_2, P_2}^{(n)}(f_{U^{(n)}, f_{U^{(n)}}^{(n)}(X^n)}^{(n)}(X^n)).$$

The set of such (R_1, R_2) is denoted as $\mathcal{R}^{(\infty)}(\Theta_1, \Theta_2)$.

Theorem 7. $\mathcal{R}^{(\infty)}(\Theta_1, \Theta_2) = \text{cl}(\overline{\mathcal{R}}(\Theta_1, \Theta_2))$.

Remark 2. Remark 1 is applicable here as well.

Proof of Theorem 7. Let Z_1 and Z_2 be jointly distributed with X such that for any $(D_1, P_1) \in \Theta_1$ and $(D_2, P_2) \in \Theta_2$, there exist $p_{\hat{X}_{1,D_1,P_1}|Z_1}$ and $p_{\hat{X}_{2,D_2,P_2}|Z_2}$ satisfying $\mathbb{E}[\Delta(X, \hat{X}_{1,D_1,P_1})] \leq D_1$, $\mathbb{E}[\Delta(X, \hat{X}_{2,D_2,P_2})] \leq D_2$, $d(p_X, p_{\hat{X}_{1,D_1,P_1}}) \leq P_1$, and $d(p_X, p_{\hat{X}_{2,D_2,P_2}}) \leq P_2$. Construct

$$p_{Z_1^n Z_2^n | X^n} \triangleq \prod_{i=1}^n p_{Z_1(i) Z_2(i) | X(i)}$$

with $p_{Z_1(i) Z_2(i) | X(i)} = p_{Z_1 Z_2 | X}$, $i = 1, \dots, n$. It follows by the strong functional representation lemma that there exist a random variable $V_1^{(n)}$, independent of X^n , and a deterministic function ϕ_1 such that $Z_1^n = \phi_1(X^n, V_1^{(n)})$ and $H(\phi_1(X^n, V_1^{(n)}) | V_1^{(n)}) \leq I(X^n; Z_1^n) + \log(I(X^n; Z_1^n) + 1) + 4$; moreover, there exist a random variable $V_2^{(n)}$, independent of $(X^n, V_1^{(n)})$, and a deterministic function ϕ_2 such that $Z_2^n = \phi_2(X^n, Z_1^n, V_2^{(n)})$ and $H(\phi_2(X^n, Z_1^n, V_2^{(n)}) | Z_1^n, V_2^{(n)}) \leq I(X^n; Z_2^n | Z_1^n) + \log(I(X^n; Z_2^n | Z_1^n) + 1) + 4$. So with $(V_1^{(n)}, V_2^{(n)})$ available at both the encoder and the decoder, we can use a class of prefix-free binary codes indexed by $V_1^{(n)}$ with the expected codeword length no greater than $I(X^n; Z_1^n) + \log(I(X^n; Z_1^n) + 1) + 5$ to lossless represent Z_1^n and then use a class of prefix-free binary codes indexed by $(Z_1^n, V_2^{(n)})$ with the expected codeword length no greater than $I(X^n; Z_2^n | Z_1^n) + \log(I(X^n; Z_2^n | Z_1^n) + 1) + 5$ to lossless represent Z_2^n .

Note that in the first stage we can send the codeword used to represent Z_1^n and with a certain probability the codeword used to represent Z_2^n . Moreover, by the functional representation lemma, there exist random variables V_{1,D_1,P_1} and V_{2,D_2,P_2} , independent of $(X^n, V_1^{(n)}, V_2^{(n)})$, and deterministic functions ψ_{1,D_1,P_1} and ψ_{2,D_2,P_2} such that $p_{\psi_{1,D_1,P_1}(Z_1(i), V_{1,D_1,P_1}) | Z_1(i)} = p_{\hat{X}_{1,D_1,P_1} | Z_1}$ and $p_{\psi_{2,D_2,P_2}(Z_2(i), V_{2,D_2,P_2}) | Z_2(i)} = p_{\hat{X}_{2,D_2,P_2} | Z_2}$. Define $\hat{X}_{1,D_1,P_1}(i) = \psi_{1,D_1,P_1}(Z_1(i), V_{1,D_1,P_1})$ and $\hat{X}_{2,D_2,P_2}(i) = \psi_{2,D_2,P_2}(Z_2(i), V_{2,D_2,P_2})$, $i = 1, \dots, n$. It is easy to verify that

$$\begin{aligned} \frac{1}{n} \sum_{i=1}^n \mathbb{E}[\Delta(X(i), \hat{X}_{k,D_k,P_k}(i))] &= \mathbb{E}[\Delta(X, \hat{X}_{k,D_k,P_k})] \leq D_k, \quad k = 1, 2, \\ d\left(p_X, \frac{1}{n} \sum_{i=1}^n p_{\hat{X}_{k,D_k,P_k}(i)}\right) &= d(p_X, p_{\hat{X}_{k,D_k,P_k}}) \leq P_k, \quad k = 1, 2. \end{aligned}$$

Furthermore,

$$\begin{aligned} &\frac{1}{n} I(X^n; Z_1^n) + \frac{1}{n} \log(I(X^n; Z_1^n) + 1) + \frac{5}{n} \\ &= I(X; Z_1) + \frac{1}{n} \log(nI(X; Z_1) + 1) + \frac{5}{n} \\ &\xrightarrow{n \rightarrow \infty} I(X; Z_1) \end{aligned}$$

and

$$\begin{aligned} &\frac{1}{n} I(X^n; Z_1^n) + \frac{1}{n} \log(I(X^n; Z_1^n) + 1) + \frac{5}{n} + \frac{1}{n} I(X^n; Z_2^n | Z_1^n) + \frac{1}{n} \log(I(X^n; Z_2^n | Z_1^n) + 1) + \frac{5}{n} \\ &= \frac{1}{n} I(X^n; Z_1^n, Z_2^n) + \frac{1}{n} \log(I(X^n; Z_1^n) + 1) + \frac{1}{n} \log(I(X^n; Z_2^n | Z_1^n) + 1) + \frac{10}{n} \\ &= I(X; Z_1, Z_2) + \frac{1}{n} \log(nI(X; Z_1) + 1) + \frac{1}{n} \log(nI(X; Z_2 | Z_1) + 1) + \frac{10}{n} \\ &\xrightarrow{n \rightarrow \infty} I(X; Z_1, Z_2). \end{aligned}$$

This proves that $\text{cl}(\overline{\mathcal{R}}(\Theta_1, \Theta_2)) \subseteq \mathcal{R}^{(\infty)}(\Theta_1, \Theta_2)$.

For any random variable $U^{(n)}$, encoding functions $f_{U^{(n)}}^{(n)} : \mathcal{X}^n \rightarrow \mathcal{C}_{U^{(n)}}^{(n)}$, $f_{U^{(n)}, f_{U^{(n)}}^{(n)}(X^n)}^{(n)} : \mathcal{X}^n \rightarrow \mathcal{C}_{U^{(n)}, f_{U^{(n)}}^{(n)}(X^n)}^{(n)}$ and decoding functions $g_{U^{(n)}, D_1, P_1}^{(n)} : \mathcal{C}_{U^{(n)}}^{(n)} \rightarrow \hat{\mathcal{X}}^n$, $(D_1, P_1) \in \Theta_1$, $g_{U^{(n)}, f_{U^{(n)}}^{(n)}(X^n), D_2, P_2}^{(n)} : \mathcal{C}_{U^{(n)}, f_{U^{(n)}}^{(n)}(X^n)} \rightarrow \hat{\mathcal{X}}^n$, $(D_2, P_2) \in \Theta_2$, satisfying (33) and (34), we have

$$\begin{aligned}
\frac{1}{n} \mathbb{E}[\ell(f_{U^{(n)}}^{(n)}(X^n))] &\geq \frac{1}{n} H(f_{U^{(n)}}^{(n)}(X^n) | U^{(n)}) \\
&= \frac{1}{n} I(X^n; f_{U^{(n)}}^{(n)}(X^n) | U^{(n)}) \\
&= \frac{1}{n} I(X^n; f_{U^{(n)}}^{(n)}(X^n), U^{(n)}) \\
&= \frac{1}{n} \sum_{i=1}^n I(X(i); f_{U^{(n)}}^{(n)}(X^n), U^{(n)} | X^{i-1}) \\
&= \frac{1}{n} \sum_{i=1}^n I(X(i); f_{U^{(n)}}^{(n)}(X^n), U^{(n)}, X^{i-1}) \\
&\geq \frac{1}{n} \sum_{i=1}^n I(X(i); f_{U^{(n)}}^{(n)}(X^n), U^{(n)}) \\
&= I(X(T); f_{U^{(n)}}^{(n)}(X^n), U^{(n)} | T) \\
&= I(X(T); f_{U^{(n)}}^{(n)}(X^n), U^{(n)}, T) \\
&= I(X(T); Z_1)
\end{aligned}$$

and

$$\begin{aligned}
&\frac{1}{n} \mathbb{E}[\ell(f_{U^{(n)}}^{(n)}(X^n))] + \frac{1}{n} \mathbb{E}[\ell(f_{U^{(n)}, f_{U^{(n)}}^{(n)}(X^n)}^{(n)}(X^n))] \\
&\geq \frac{1}{n} H(f_{U^{(n)}}^{(n)}(X^n) | U^{(n)}) + \frac{1}{n} H(f_{U^{(n)}, f_{U^{(n)}}^{(n)}(X^n)}^{(n)}(X^n) | U^{(n)}, f_{U^{(n)}}^{(n)}(X^n)) \\
&\geq \frac{1}{n} I(X^n; f_{U^{(n)}}^{(n)}(X^n) | U^{(n)}) + \frac{1}{n} I(X^n; f_{U^{(n)}, f_{U^{(n)}}^{(n)}(X^n)}^{(n)}(X^n) | U^{(n)}, f_{U^{(n)}}^{(n)}(X^n)) \\
&= \frac{1}{n} I(X^n; f_{U^{(n)}}^{(n)}(X^n), f_{U^{(n)}, f_{U^{(n)}}^{(n)}(X^n)}^{(n)}(X^n) | U^{(n)}) \\
&= \frac{1}{n} I(X^n; f_{U^{(n)}}^{(n)}(X^n), f_{U^{(n)}, f_{U^{(n)}}^{(n)}(X^n)}^{(n)}(X^n), U^{(n)}) \\
&= \frac{1}{n} \sum_{i=1}^n I(X(i); f_{U^{(n)}}^{(n)}(X^n), f_{U^{(n)}, f_{U^{(n)}}^{(n)}(X^n)}^{(n)}(X^n), U^{(n)} | X^{i-1}) \\
&= \frac{1}{n} \sum_{i=1}^n I(X(i); f_{U^{(n)}}^{(n)}(X^n), f_{U^{(n)}, f_{U^{(n)}}^{(n)}(X^n)}^{(n)}(X^n), U^{(n)}, X^{i-1}) \\
&\geq \frac{1}{n} \sum_{i=1}^n I(X(i); f_{U^{(n)}}^{(n)}(X^n), f_{U^{(n)}, f_{U^{(n)}}^{(n)}(X^n)}^{(n)}(X^n), U^{(n)}) \\
&= I(X(T); f_{U^{(n)}}^{(n)}(X^n), f_{U^{(n)}, f_{U^{(n)}}^{(n)}(X^n)}^{(n)}(X^n), U^{(n)} | T) \\
&= I(X(T); f_{U^{(n)}}^{(n)}(X^n), f_{U^{(n)}, f_{U^{(n)}}^{(n)}(X^n)}^{(n)}(X^n), U^{(n)}, T) \\
&= I(X(T); Z_1, Z_2),
\end{aligned}$$

where T is uniformly distributed over $\{1, \dots, n\}$ and is independent of $(X^n, U^{(n)})$, and we define $Z_1 = (f_{U^{(n)}}^{(n)}(X^n), U^{(n)}, T)$ and $Z_2 = (f_{U^{(n)}, f_{U^{(n)}}^{(n)}(X^n)}^{(n)}(X^n), U^{(n)}, T)$. Since

$$p_{X(T)} = p_X,$$

$$\mathbb{E}[\Delta(X(T), \hat{X}_{k, D_k, P_k}(T))] = \frac{1}{n} \sum_{i=1}^n \mathbb{E}[\Delta(X(i), \hat{X}_{k, D_k, P_k}(i))] \leq D_k, \quad k = 1, 2,$$

$$d(p_{X(T)}, p_{\hat{X}_{k, D_k, P_k}(T)}) = d\left(p_X, \frac{1}{n} \sum_{i=1}^n p_{\hat{X}_{k, D_k, P_k}(i)}\right) \leq P_k, \quad k = 1, 2,$$

and $\hat{X}_{k, D_k, P_k}(T)$ is a function of Z_k , $k = 1, 2$, we must have $(R_1, R_2) \in \overline{\mathcal{R}}(\Theta_1, \Theta_2)$ for any (R_1, R_2) with $R_1 \geq \frac{1}{n} \mathbb{E}[\ell(f_U^{(n)}(X^n))]$ and $R_2 \geq \frac{1}{n} \mathbb{E}[\ell(f_{U, f_U^{(n)}(X^n)}^{(n)}(X^n))]$. This completes the proof. \square

Definition 8. We say that Θ_1 can be successively refined to Θ_2 if $(R(\Theta_1), R(\Theta_2) - R(\Theta_1)) \in \text{cl}(\overline{\mathcal{R}}(\Theta_1, \Theta_2))$

Remark 3. To show the asymptotic feasibility of successive refinement from Θ_1 to Θ_2 , it suffices to find $p_{Z_1, Z_2|X}$ such that

$$I(X; Z_1) = R(\Theta_1), \quad I(X; Z_1, Z_2) = R(\Theta_2),$$

and for any $(D_1, P_1) \in \Theta_1$ and $(D_2, P_2) \in \Theta_2$, there exists

$$p_{\hat{X}_{1, D_1, P_1}|Z_1} \quad \text{and} \quad p_{\hat{X}_{2, D_2, P_2}|Z_2}$$

satisfying

$$\begin{aligned} \mathbb{E}[\Delta(X; \hat{X}_{1, D_1, P_1})] &\leq D_1, & \mathbb{E}[\Delta(X; \hat{X}_{2, D_2, P_2})] &\leq D_2, \\ d(p_X, p_{\hat{X}_{1, D_1, P_1}}) &\leq P_1, & d(p_X, p_{\hat{X}_{2, D_2, P_2}}) &\leq P_2. \end{aligned}$$

In the Gaussian case, it is easy to show that successive refinement from Θ_1 to Θ_2 is always asymptotically feasible for $R(\Theta_2) \geq R(\Theta_1)$.

Theorem 8. Let $X \sim \mathcal{N}(\mu_X, \sigma_X^2)$ be a scalar Gaussian source and assume MSE and $W_2^2(\cdot, \cdot)$ losses. Let Θ_1 and Θ_2 be arbitrary non-empty sets of (D, P) pairs with $R(\Theta_1) \leq R(\Theta_2)$. Then $(R(\Theta_1), R(\Theta_2) - R(\Theta_1)) \in \mathcal{R}^{(\infty)}(\Theta_1, \Theta_2)$, i.e., successive refinement from Θ_1 to Θ_2 is feasible.

Proof of Theorem 8. Let $Z_2 = Z_1 + N_1$ and $X = Z_2 + N_2$, where

$$\begin{aligned} Z_1 &\sim \mathcal{N}(\mu_X, \sigma_X^2(1 - 2^{-2R(\Theta_1)})), \\ N_1 &\sim \mathcal{N}(0, \sigma_X^2(2^{-2R(\Theta_1)} - 2^{-2R(\Theta_2)})), \\ N_2 &\sim \mathcal{N}(0, \sigma_X^2 2^{-2R(\Theta_2)}) \end{aligned}$$

are mutually independent. It is easy to verify that $I(X; Z_1) = R(\Theta_1)$ and $I(X; Z_1, Z_2) = I(X; Z_2) = R(\Theta_2)$. In view of Theorem 3, we have $\Theta_i \subseteq \Omega(p_{Z_i|X}) = \Omega(R(\Theta_i))$, $i = 1, 2$. So successive refinement from Θ_1 to Θ_2 is indeed asymptotically feasible. \square

Theorem 9 (Approximate refinability under the iRDPF). Assume MSE loss and any perception measure $d(\cdot, \cdot)$. Let m be the dimension of X and

$$\delta_R(\sigma_N^2) = R(\Theta_1) - R\left(\frac{\sigma_X^2 \sigma_N^2}{\sigma_X^2 + \sigma_N^2}, \infty\right) + \frac{m}{2} \log \frac{(D_1^* + \sigma_N^2)(D_2^* + \sigma_N^2)}{\sigma_N^4},$$

where

$$\begin{aligned} D_1^* &= \inf\{D'_1 : (D'_1, P'_1) \in \Theta_1 \text{ for some } P'_1\}, \\ D_2^* &= \inf\{D'_2 : (D'_2, P'_2) \in \Theta_1 \text{ for some } P'_2\}. \end{aligned}$$

Then for any non-empty Θ_1 and Θ_2 ,

$$(R(\Theta_1), R(\Theta_2) - R(\Theta_1) + \inf_{\sigma_N^2 > 0} \delta_R(\sigma_N^2)) \in \mathcal{R}^{(\infty)}(\Theta_1, \Theta_2).$$

Remark 4. We have

$$\delta_R\left(\frac{\sigma_X^2 D_1^*}{\sigma_X^2 - D_1^*}\right) = R(\Theta_1) - R(D_1^*, \infty) + \frac{m}{2} \log \frac{(\sigma_X^2 (D_1^* + D_2^*) - D_1^* D_2^*)(2\sigma_X^2 - D_1^*)}{\sigma_X^4 D_1^*}.$$

In particular, $\delta_R\left(\frac{\sigma_X^2 D_1^*}{\sigma_X^2 - D_1^*}\right) \leq m$ when $R(\Theta_1) = R(D_1^*, \infty)$ and $D_2^* \leq D_1^*$. In the scalar case, this shows that the penalty for refinement (as opposed to sending all bits at once) is not more than 1 bit.

Proof of Theorem 9. This proof is an adaptation of the result from Lastras and Berger [18].

For any $\epsilon > 0$, we can find Z_k with $I(X; Z_k) \leq R(\Theta_k) + \epsilon$ such that for any $(D_k, P_k) \in \Theta_k$, there exists $p_{\hat{X}_{k,D_k,P_k}|Z_k}$ satisfying $\mathbb{E}[\|X - \hat{X}_{k,D_k,P_k}\|^2] \leq D_k$ and $d(p_X, p_{\hat{X}_{k,D_k,P_k}}) \leq P_k$, $k = 1, 2$. We define X , Z_1 , and Z_2 in the same probability space such that $Z_1 \leftrightarrow X \leftrightarrow Z_2$ form a Markov chain. It suffices to show that $I(X; Z_1, Z_2) \leq R(\Theta_2) + \delta_R(\sigma_N^2) + 2\epsilon$ for any $\sigma_N^2 > 0$.

Let $N \sim \mathcal{N}(0, \frac{\sigma_N^2}{m} I_m)$ be an m -dimensional (multivariate) Gaussian random variable independent of (X, Z_1, Z_2) . We have

$$\begin{aligned} I(X; Z_1, Z_2) - I(X; Z_2) &= I(X; Z_1|Z_2) \\ &\leq I(X; Z_1, X + N|Z_2) \\ &= I(X; X + N|Z_2) + I(X; Z_1|Z_2, X + N). \end{aligned} \quad (35)$$

Note that

$$\begin{aligned} I(X; X + N|Z_2) &= I(X - \mathbb{E}[X|Z_2]; X - \mathbb{E}[X|Z_2] + N|Z_2) \\ &\leq I(Z_2, X - \mathbb{E}[X|Z_2]; X - \mathbb{E}[X|Z_2] + N) \\ &= I(X - \mathbb{E}[X|Z_2]; X - \mathbb{E}[X|Z_2] + N) \\ &\leq \frac{m}{2} \log \frac{D_2^* + \sigma_N^2}{\sigma_N^2} \end{aligned} \quad (36)$$

and

$$\begin{aligned} &I(X; Z_1|Z_2, X + N) \\ &\leq I(X, Z_2; Z_1|X + N) \\ &= I(X; Z_1|X + N) \\ &= I(X; Z_1, X + N) - I(X; X + N) \\ &= I(X; X + N|Z_1) + I(X; Z_1) - I(X; X + N) \\ &\leq I(X; X + N|Z_1) + R(\Theta_1) + \epsilon - I(X; X + N) \\ &\stackrel{(\beta)}{\leq} I(X; X + N|Z_1) + R(\Theta_1) + \epsilon - R\left(\frac{\sigma_X^2 \sigma_N^2}{\sigma_X^2 + \sigma_N^2}, \infty\right) \\ &= I(X - \mathbb{E}[X|Z_1]; X - \mathbb{E}[X|Z_1] + N|Z_1) + R(\Theta_1) - R\left(\frac{\sigma_X^2 \sigma_N^2}{\sigma_X^2 + \sigma_N^2}, \infty\right) + \epsilon \\ &\leq I(Z_1, X - \mathbb{E}[X|Z_1]; X - \mathbb{E}[X|Z_1] + N) + R(\Theta_1) - R\left(\frac{\sigma_X^2 \sigma_N^2}{\sigma_X^2 + \sigma_N^2}, \infty\right) + \epsilon \\ &= I(X - \mathbb{E}[X|Z_1]; X - \mathbb{E}[X|Z_1] + N) + R(\Theta_1) - R\left(\frac{\sigma_X^2 \sigma_N^2}{\sigma_X^2 + \sigma_N^2}, \infty\right) + \epsilon \\ &\leq \frac{m}{2} \log \frac{D_1^* + \sigma_N^2}{\sigma_N^2} + R(\Theta_1) - R\left(\frac{\sigma_X^2 \sigma_N^2}{\sigma_X^2 + \sigma_N^2}, \infty\right) + \epsilon, \end{aligned} \quad (37)$$

where (β) is because $\mathbb{E}[\|X - \frac{\sigma_X^2}{\sigma_X^2 + \sigma_N^2}(X + N) - \frac{\sigma_N^2}{\sigma_X^2 + \sigma_N^2}\mu_X\|^2] = \frac{\sigma_X^2 \sigma_N^2}{\sigma_X^2 + \sigma_N^2}$ and consequently $I(X; X + N) \geq R\left(\frac{\sigma_X^2 \sigma_N^2}{\sigma_X^2 + \sigma_N^2}, \infty\right)$. Substituting (36) and (37) into (35) gives

$$I(X; Z_1, Z_2) - I(X; Z_2) \leq \delta_R(\sigma_N^2) + \epsilon,$$

which further implies

$$I(X; Z_1, Z_2) \leq R(\Theta_2) + \delta_R(\sigma_N^2) + 2\epsilon.$$

This completes the proof. \square

B Experiments

Training lasted 30 epochs for MNIST and 80 epochs for SVHN, and alternates between training the encoder and decoder with the critic fixed and training the critic with the encoder and decode fixed. The learning rate was decayed by a factor of 5 after 20 epochs for MNIST, and after 25 epochs for SVHN. All models were trained with the Adam optimizer. The batch size used was 64. All training was performed on a Tesla V100 GPU. Training a single model takes about 10 minutes and 30 minutes for MNIST and SVHN, respectively. We used the standard train/test splits.

B.1 Comparison of Quantizers

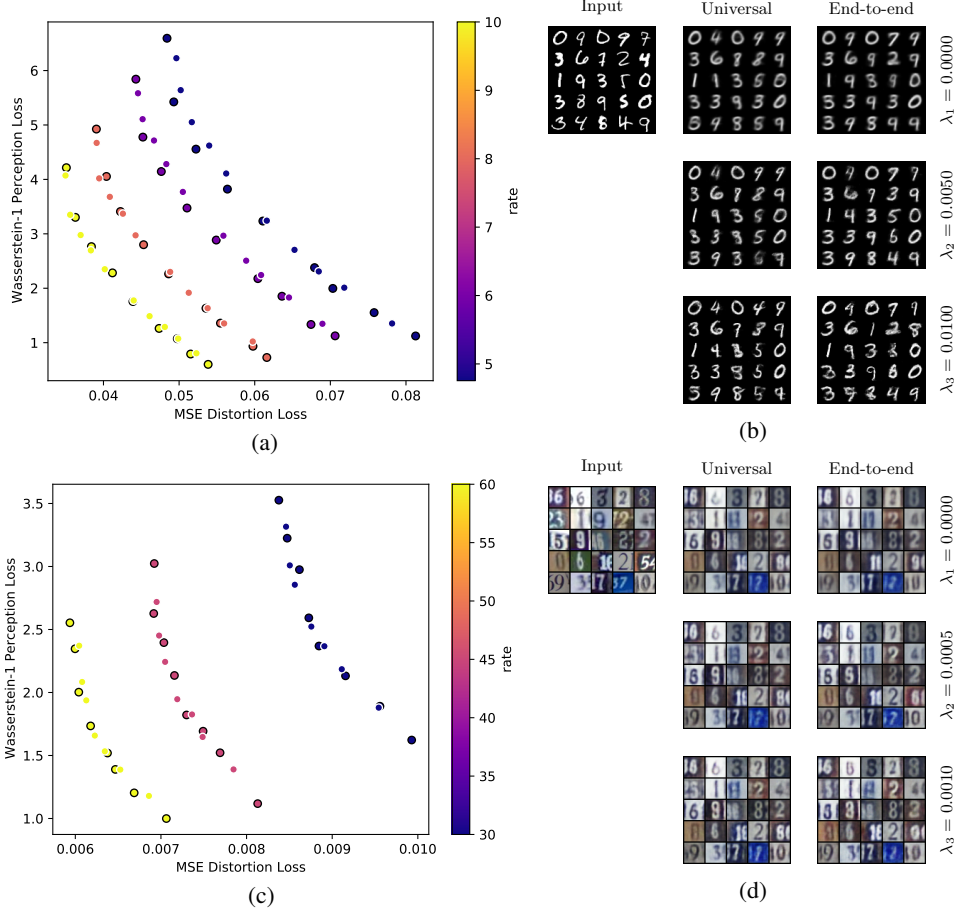


Figure 5: (a) (c) Rate-distortion-perception tradeoffs for NQ. (b) (d) The visual quality of both the end-to-end and universal models are on average comparable for each λ_i (MNIST: $R = 6$, SVHN: $R = 60$.)

Let \mathcal{C} be the set of quantization centers, each containing L levels distributed uniformly between $[-1, +1]$ along each dimension d . Let x be the input and $f(x)$ the output of the encoder before quantization. We compare the performance of deterministic quantization (DQ), universal quantization (UQ), and noisy quantization (NQ). All quantizers use a soft gradient estimator (equation (3) of Mentzer et al. [21]) during backpropagation.

Deterministic quantization (DQ). The sender computes

$$z = \arg \min_{c \in \mathcal{C}} \|f(x) - c\|$$

and sends z to the receiver. The receiver decodes the image by passing z through the decoder. This is the most straightforward method of quantization but lacks the stochasticity required to train an effective generative model.

Quantization with noise added (NQ). The sender computes

$$z = \arg \min_{c \in \mathcal{C}} \|f(x) - c\|$$

and sends z to the receiver. The receiver samples $u \sim U[-1/(L-1), +1/(L-1)]^d$ and decodes the image by passing $z + u$ through the decoder. Note that there is no information loss as the noise range is almost surely below the quantization interval. This scheme was used by Blau and Michaeli [5].

Universal quantization (UQ) [30, 42]. We assume the sender and receiver have access to $u \sim U[-1/(L-1), +1/(L-1)]^d$. The sender computes

$$z = \arg \min_{c \in \mathcal{C}} \|f(x) + u - c\|$$

and sends z to the receiver. The receiver decodes the image by passing $z - u$ through the decoder. This quantization scheme produces stochastic input for the decoder while reducing the quantization error incurred by NQ. This is also known as a subtractive dither [12, 29] in literature.

We demonstrate in Figure 5 that the NQ scheme is still able to produce universal representations within the operational tradeoff it achieves. The results of the comparison when optimizing only for MSE loss are given in Table 1. Both DQ and UQ perform better than NQ. Although DQ performs slightly better, UQ is still highly effective.

Table 1: Comparison of MSE distortion losses using deterministic quantization (DQ), universal quantization (UQ), and noisy quantization (NQ) when optimizing an end-to-end model only for distortion loss ($\lambda = 0$) on MNIST.

R	MSE (DQ)	MSE (UQ)	MSE (NQ)
4.75	0.0442	0.0459	0.0484
6	0.0412	0.0426	0.0443
8	0.0358	0.0362	0.0391
10	0.0315	0.0324	0.0351

B.2 Error Intervals

We provide error intervals across 5 trials for a subset of the universality experiments given in Figure 4 on MNIST here. Each trial consists of training a new end-to-end model ($\lambda = 0.015$, $R = 4.75$), then using the resultant encoder to train universal models across all tradeoff points. The results are very consistent across each trial.

Table 2: MSE distortion losses across 5 trials.

λ	0.0000	0.0025	0.0040	0.0050	0.0060	0.0080	0.0090	0.0100	0.0110	0.0130
max	0.0470	0.0477	0.0493	0.0507	0.0531	0.0583	0.0614	0.0648	0.0681	0.0729
min	0.0466	0.0474	0.0490	0.0504	0.0526	0.0577	0.0606	0.0640	0.0665	0.0715
average	0.0468	0.0475	0.0491	0.0506	0.0528	0.0579	0.0609	0.0643	0.0670	0.0720

Table 3: Wasserstein-1 perception losses across 5 trials.

λ	0.0000	0.0025	0.0040	0.0050	0.0060	0.0080	0.0090	0.0100	0.0110	0.0130
max	5.8014	5.1464	4.6482	4.2692	3.7672	2.9855	2.5596	2.1221	1.9033	1.3256
min	5.5787	5.0612	4.5815	4.1812	3.7576	2.8928	2.5105	2.0020	1.6842	1.1958
average	5.7123	5.1087	4.6177	4.2211	3.7636	2.9446	2.5259	2.0778	1.8296	1.2718

B.3 Refinement Experiments

So far, we have enforced the decoders in universal models to use only the representations produced by the universal encoder, producing a tradeoff curve along perception and distortion at fixed rate. We now consider the scenario where the rate is varied by designing *refinement* models which generalize the universal models in the previous section by taking in extra bits through a (trainable) refining encoder in addition to the bits produced by the initial encoder.

Like the universal models, training the refinement models is broken into two analogous stages. The objective and procedure of the first stage is identical to that of the universal models and produces a universal encoder f to be used across multiple models with frozen weights, and a low-rate decoder g . In the second stage, the refinement model introduces a new high-rate decoder g_1^+ building upon representations from both the universal encoder f and a secondary refining encoder f_1^+ . The refining encoder and decoder are both trained along with a critic h_1^+ , while the universal encoder is held fixed. We use the alternating training procedure as with the universal models. Bits are sent in two stages so that either low rate or high rate reconstructions

$$\hat{X}_1^{(1)} = g(f(X)), \quad (38)$$

$$\hat{X}_1^{(2)} = g_1^+(f(X), f_1^+(X)) \quad (39)$$

are possible. One may take the view that f_1^+ will embed auxiliary details about the input to supplement the information extracted by f . Since f is held fixed while g_1^+ is being trained, we expect that there should be a performance gap between the refinement model and an end-to-end model with full flexibility in training an encoder. In Figure 6, we find that the gap is not sizeable in practice, with the visual quality of the refinement models similar to the end-to-end models of the same rate.

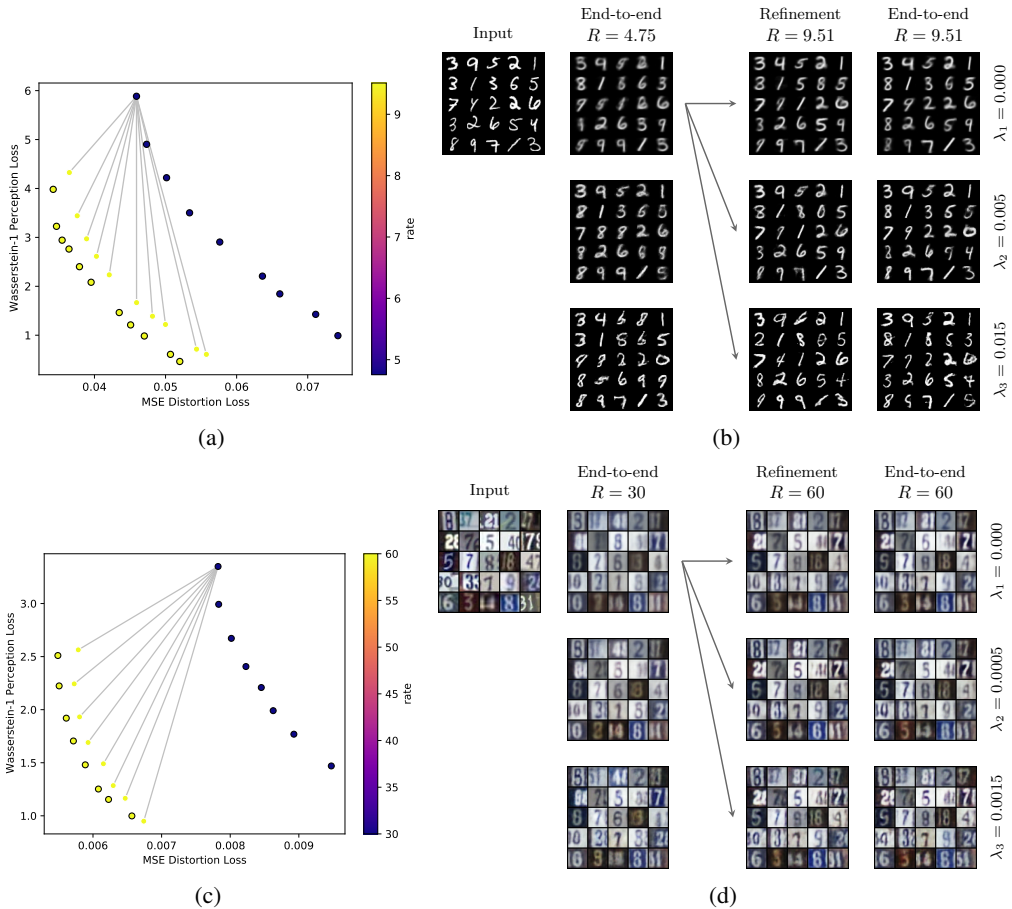


Figure 6: (a) (c) Rate refinability of MNIST and SVHN. Points with black outline are losses for the end-to-end models. Points without outline are the losses for the refinement models, which were trained with a encoder optimized for only distortion loss ($\lambda = 0$). For fair comparison, the parameter count of an end-to-end encoder at high rate is approximately equal to the sum of the parameter counts for the universal encoder and refining encoder in the refinement model. Refinement from $\lambda = 0$ performs closest to end-to-end models of the same rate, but any $\lambda > 0$ can be refined. (b) (d) Outputs of selected models. Visual reconstruction of refinement models is similar to that of high-rate end-to-end models across all tradeoffs.

B.4 Architecture

The architectures used for the experiments are given as follows. Here each row represents a group of layers. d denotes the latent dimension and L the number of quantization levels per dimension, with $R = d \log L$. The widths of the layers may be varied for some experiments (e.g. to facilitate fair comparison in parameter count between the refinement models and end-to-end models). The quantizer performs hard nearest-neighbour quantization on the forward pass and uses a soft relaxation given by Equation (3) in [21] during the backward pass. The bin centers for quantization are spaced evenly in $[-1, 1]$ for each dimension. The type of compression systems are denoted by E for end-to-end, U for (perception-distortion) universal and R for refinement.

B.4.1 MNIST

The universality experiments build off of the encoders produced by the end-to-end experiments of the same rate with $\lambda = 0.015$. The refinement experiment in row 2 of the right table builds off the universal encoder produced by the end-to-end model of row 1 with $\lambda = 0, 0.015$. For fair comparison, the parameter count of an end-to-end encoder at $R = 9.51$ is approximately equal to the sum of the parameter counts for the universal encoder and refining encoder in the refinement model at $R = 9.51$.

Table 4: Network and quantizer settings for MNIST. Left table: models shown in Figure 4(a). Right table: models shown in Figure 6(a).

System	R	d	L	System	R	d	L
E+U	4.75	3	3	E	4.75	3	3
E+U	6	3	4	R	9.51	3 + 3	3
E+U	8	4	4	E	9.51	6	3
E+U	10	5	4				

Table 5: The tradeoff coefficients used across all rates in each experiment for MNIST.

System	Tradeoff coefficients
E (Figure 4(a))	$\lambda = 0, 0.0033, 0.005, 0.0066, 0.008, 0.01, 0.011, 0.013, 0.015$
U (Figure 4(a))	$\lambda_i = 0, 0.0025, 0.004, 0.005, 0.006, 0.008, 0.009, 0.01, 0.011, 0.013$
E (Figure 6(a))	$\lambda = 0, 0.0033, 0.005, 0.0066, 0.008, 0.01, 0.011, 0.013, 0.015$
R (Figure 6(a))	$\lambda_i = 0, 0.0025, 0.004, 0.005, 0.006, 0.008, 0.009, 0.01, 0.013, 0.015$

Table 6: Model architectures for MNIST. l-ReLU denotes Leaky ReLU. Refer to code for parameter settings.

Encoder	Decoder
Input	Input
Flatten	Linear, BatchNorm1D, l-ReLU
Linear, BatchNorm2D, l-ReLU	Linear, BatchNorm1D, l-ReLU
Linear, BatchNorm2D, l-ReLU	Unflatten
Linear, BatchNorm2D, l-ReLU	ConvT2D, BatchNorm2D, l-ReLU
Linear, BatchNorm2D, l-ReLU	ConvT2D, BatchNorm2D, l-ReLU
Linear, BatchNorm2D, Tanh	ConvT2D, BatchNorm2D, Sigmoid
Quantizer	
	Critic
	Input
	Conv2D, l-ReLU
	Conv2D, l-ReLU
	Conv2D, l-ReLU
	Linear

Table 7: Hyperparameters used for training MNIST models across all rates, including for universal/refining encoders. α is the learning rate, (β_1, β_2) are the parameters for Adam, and λ_{GP} is the gradient penalty coefficient.

	α	β_1	β_2	λ_{GP}
Encoder	10^{-2}	0.5	0.9	-
Decoder	10^{-2}	0.5	0.9	-
Critic	2×10^{-4}	0.5	0.9	10

B.4.2 SVHN

The experiments are similar to MNIST, with the main difference being in the encoder architecture. The universality experiments build off of the encoders produced by the end-to-end experiments of the same rate with $\lambda = 0.002$. The refinement experiment in row 1 of the right table builds off the universal encoder produced by the end-to-end model of row 1 with $\lambda = 0, 0.002$. For fair comparison, the parameter count of an end-to-end encoder at $R = 60$ is approximately equal to the sum of the parameter counts for the universal encoder and refining encoder in the refinement model at $R = 30$.

Table 8: Network and quantizer settings for SVHN. Left table: models shown in Figure 4(c). Right table: models shown in Figure 6(c).

System	R	d	L	System	R	d	L
E+U	30	10	8	E	30	10	8
E+U	45	15	8	R	60	10 + 10	8
E+U	60	20	8	E	60	20	8

Table 9: The tradeoff coefficients used across all rates in each experiment for SVHN.

System	Tradeoff coefficients
E (Figure 4(c))	$\lambda = 0, 0.00025, 0.0005, 0.00075, 0.001, 0.00125, 0.0015, 0.002$
U (Figure 4(c))	$\lambda_i = 0, 0.0003, 0.0005, 0.0008, 0.001, 0.0012, 0.0017$
E (Figure 6(c))	$\lambda = 0, 0.00025, 0.0005, 0.00075, 0.001, 0.00125, 0.0015, 0.002$
R (Figure 6(c))	$\lambda_i = 0, 0.00025, 0.0005, 0.00075, 0.001, 0.00125, 0.0015, 0.002$

Table 10: Model architectures for SVHN. Refer to code for parameter settings.

Encoder	Decoder	Critic
Input	Input	Input
Conv2D, l-ReLU	Linear, BatchNorm1D, l-ReLU	Conv2D, l-ReLU
Conv2D, l-ReLU	Linear, BatchNorm1D, l-ReLU	Conv2D, l-ReLU
Conv2D, l-ReLU	Unflatten	Conv2D, l-ReLU
Flatten	ConvT2D, BatchNorm2D, l-ReLU	Linear
Linear, Tanh	ConvT2D, BatchNorm2D, l-ReLU	
Quantizer	ConvT2D, BatchNorm2D, l-ReLU	
	ConvT2D, BatchNorm2D, Sigmoid	

Table 11: Hyperparameters used for training. α is the learning rate, (β_1, β_2) are the parameters for Adam, and λ_{GP} is the gradient penalty coefficient.

	α	β_1	β_2	λ_{GP}
Encoder	10^{-4}	0.5	0.999	-
Decoder	10^{-4}	0.5	0.999	-
Critic	10^{-4}	0.5	0.999	10